U.S. Particle Accelerator School

Education in Beam Physics and Accelerator Technology

Simulations of Beam and Plasma Systems

Steven M. Lund, David Bruhwiler, Rémi Lehe, Jean-Luc Vay and Daniel Winklehner

Sponsoring University: Old Dominion University

Hampton, Virginia – January 15-26, 2018

Mesh Refinement in Field Solvers

Jean-Luc Vay

Lawrence Berkeley National Laboratory

This material is based upon work supported by the U.S. Department of Energy, Office of Science and the National Nuclear Security Administration, under Award Number(s) DE-AC02-05CH11231 and 17-SC-20-SC. Used resources of the National Energy Research Scientific Computing Center.

U.S. DEPARTMENT OF ENERGY

Office of Science

ECP EXASCALE COMPUTING PROJECT

NERSC

BERKELEY LAB

Lawrence Berkeley National Laboratory

Outline

- Why mesh refinement?
- Potential issues
- Electrostatic mesh refinement
  - spurious self-force example
  - spurious self-force mitigation
  - application to the modeling of HCX injector
- Electromagnetic mesh refinement
  - spurious reflection of waves
  - spurious reflection of waves mitigation
  - Application to the modeling beam-induced plasma wake
- Special mesh refinement for particle emission
- Summary

Why mesh refinement?

To resolve density spikes & gradients.

Injector

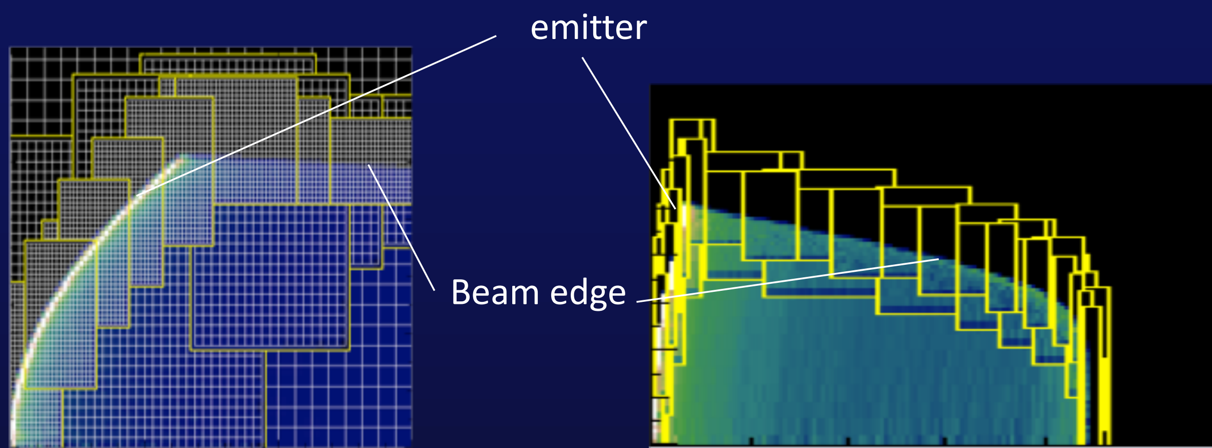

Electron cloud

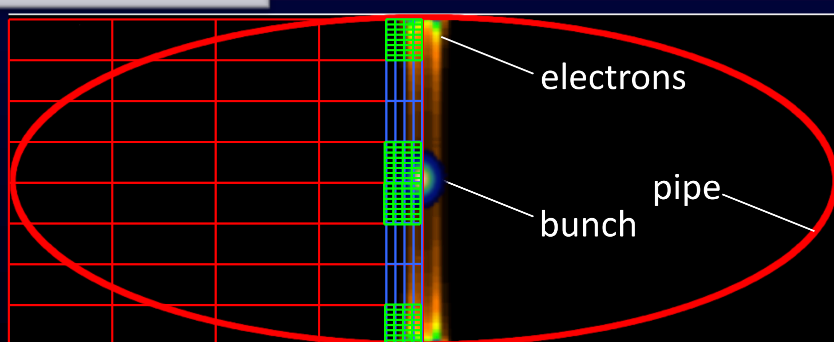

Plasma accelerator

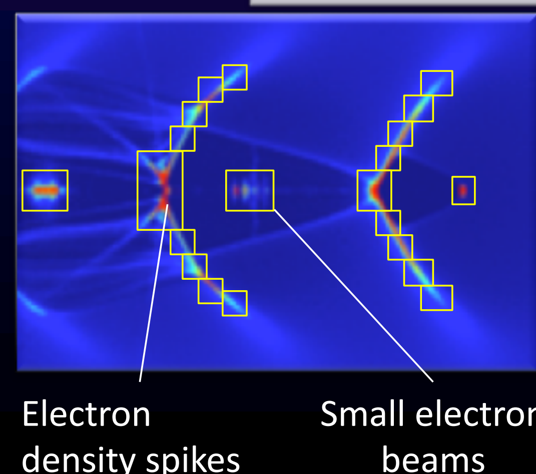

Coupling of AMR to PIC: issues

Mesh refinement implies:

➔ jump of resolution at coarse-fine interface,

➔ some procedure for coupling the solutions at the interface.

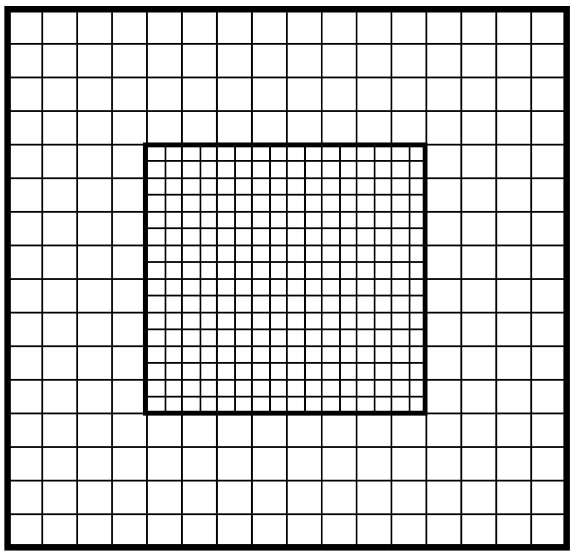

Consequences:

- loss of symmetry: self-force,
- loss of conservation laws,
- EM: waves reflection.

Electrostatic mesh refinement

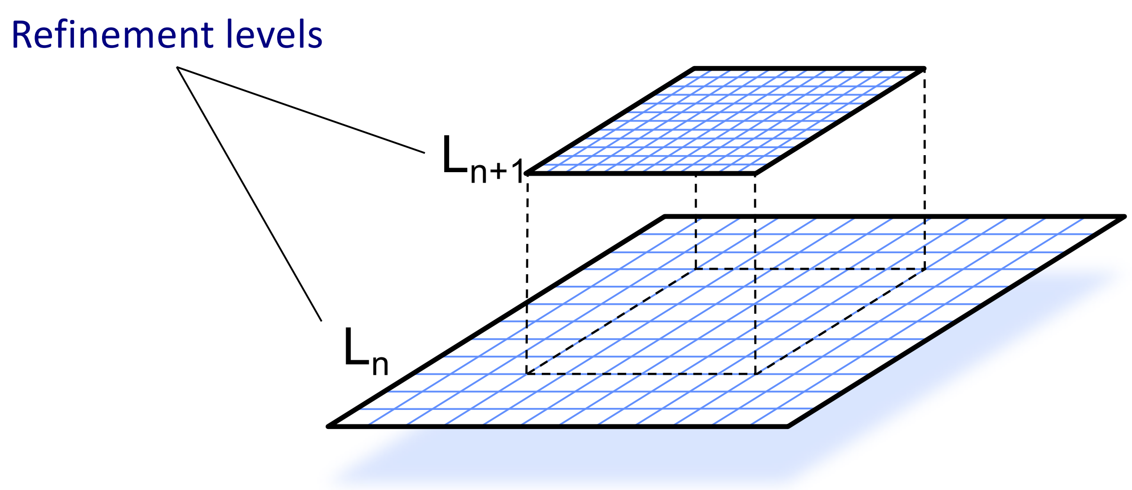

Solution to Poisson is a boundary value problem.
We can define the following simple procedure:

1. solve on coarse grid,
2. interpolate on fine grid boundaries,
3. solve on fine grid.

Electrostatic mesh refinement

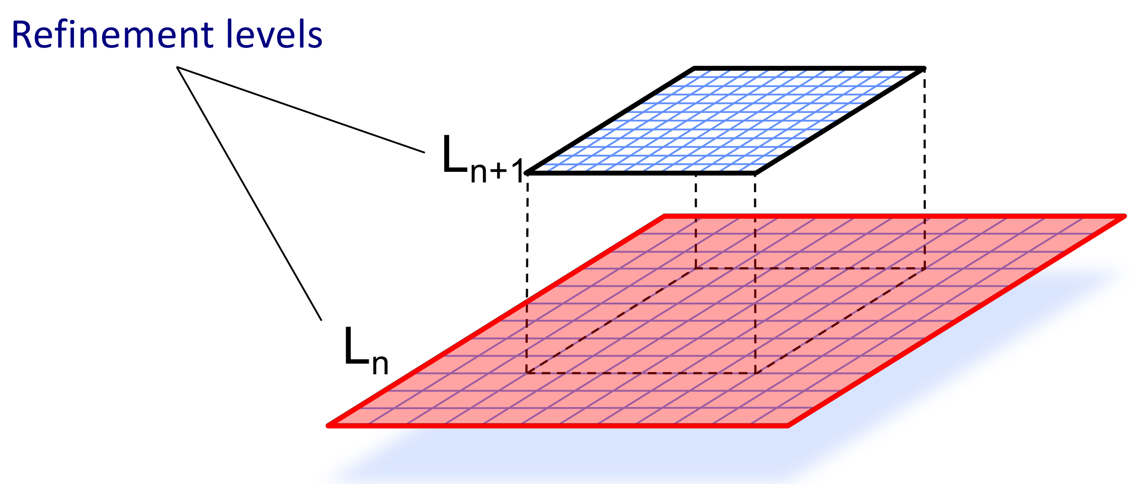

Solution to Poisson is a boundary value problem.
We can define the following simple procedure:

1. **solve on coarse grid,**
2. interpolate on fine grid boundaries,
3. solve on fine grid.

Electrostatic mesh refinement

Refinement levels

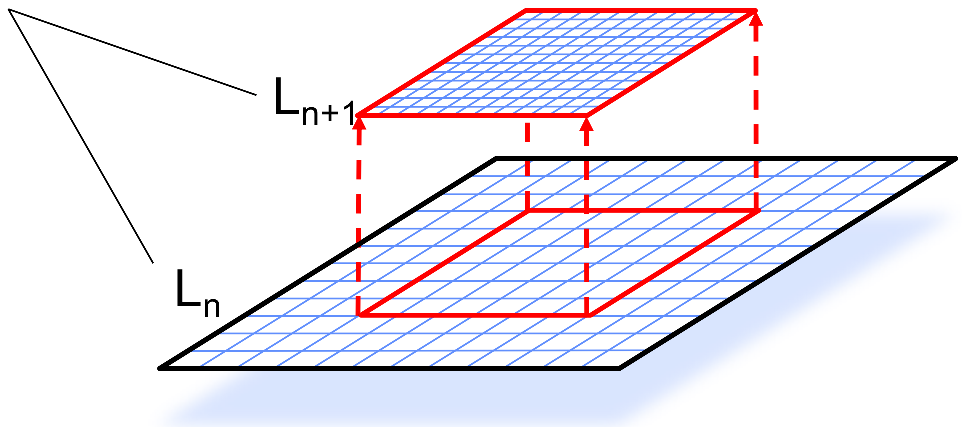

Solution to Poisson is a boundary value problem.
We can define the following simple procedure:

1. solve on coarse grid,
2. **interpolate on fine grid boundaries,**
3. solve on fine grid.

Electrostatic mesh refinement

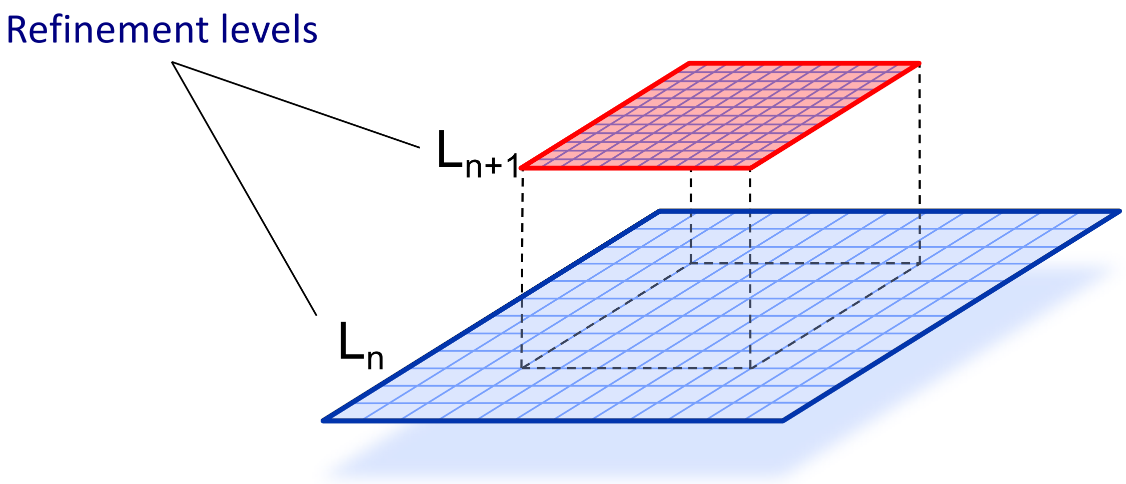

Solution to Poisson is a boundary value problem.
We can define the following simple procedure:

1. solve on coarse grid,
2. interpolate on fine grid boundaries,
3. **solve on fine grid.**

Illustration potential problem: spurious self-force

Test using script test1partin1patch.py:

- **Run with l_mr=0.**

One charged macroparticle
in a box with metallic BC

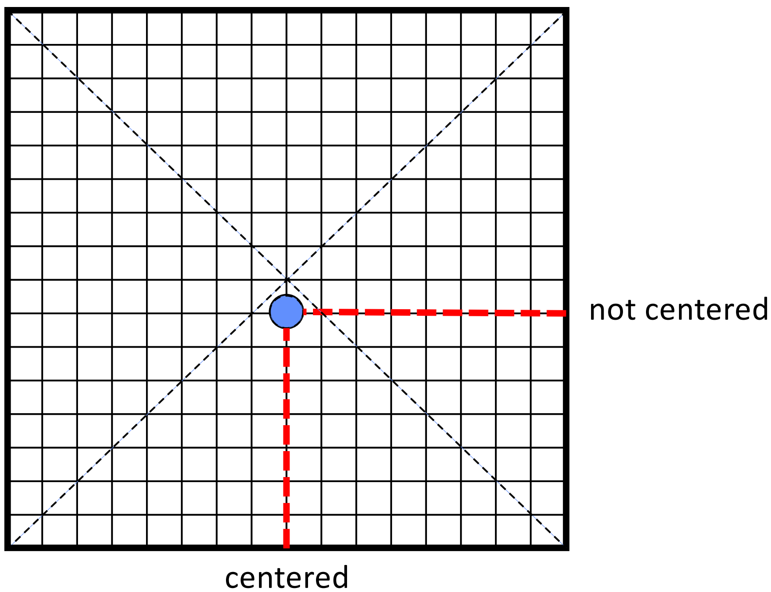

Illustration potential problem: spurious self-force

Test using script test1partin1patch.py:

- **Run with l_mr=0.**

The macroparticle is attracted by its image from the closest metallic wall.

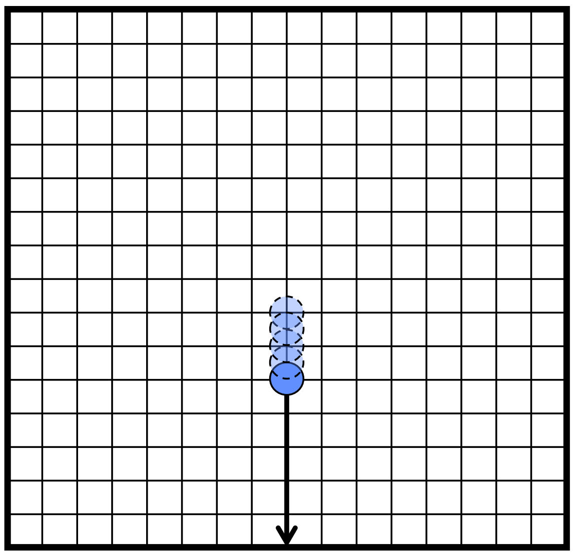

Illustration potential problem: spurious self-force

Test using script test1partin1patch.py:

- **Run with l_mr=0.**

We apply specular reflection
at the boundary.

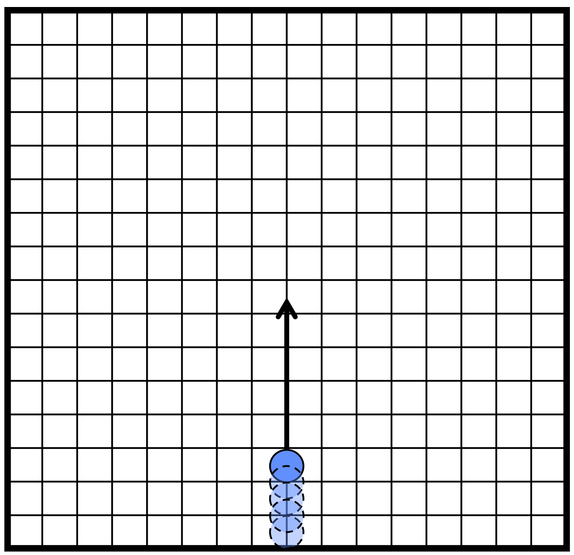

Illustration potential problem: spurious self-force

Test using script test1partin1patch.py:

- **Run with l_mr=0.**

The particle moves up and down.

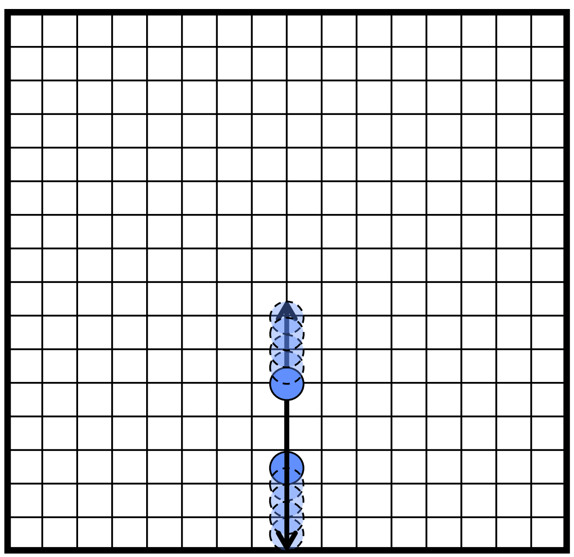

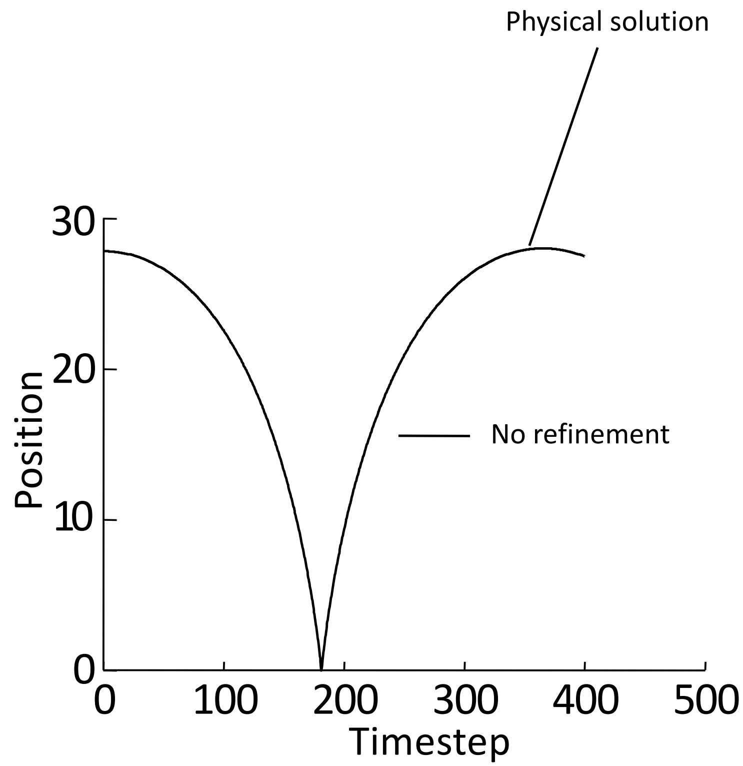

Illustration potential problem: spurious self-force

Test using script test1partin1patch.py:

- **Run with l_mr=1.**

Now add a refinement patch.

➔ Particle is trapped in patch by "spurious self-force"

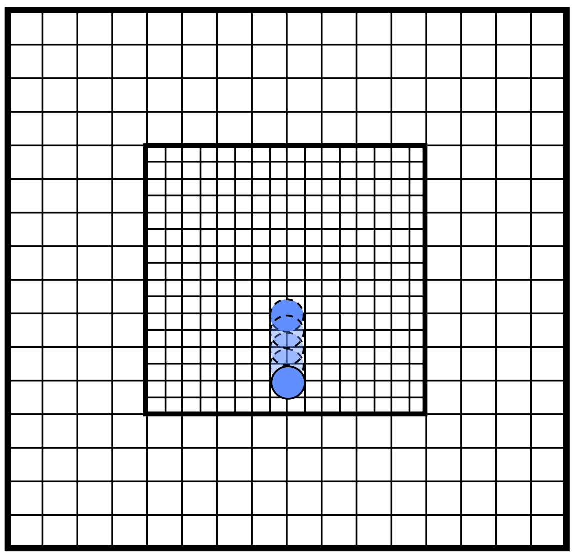

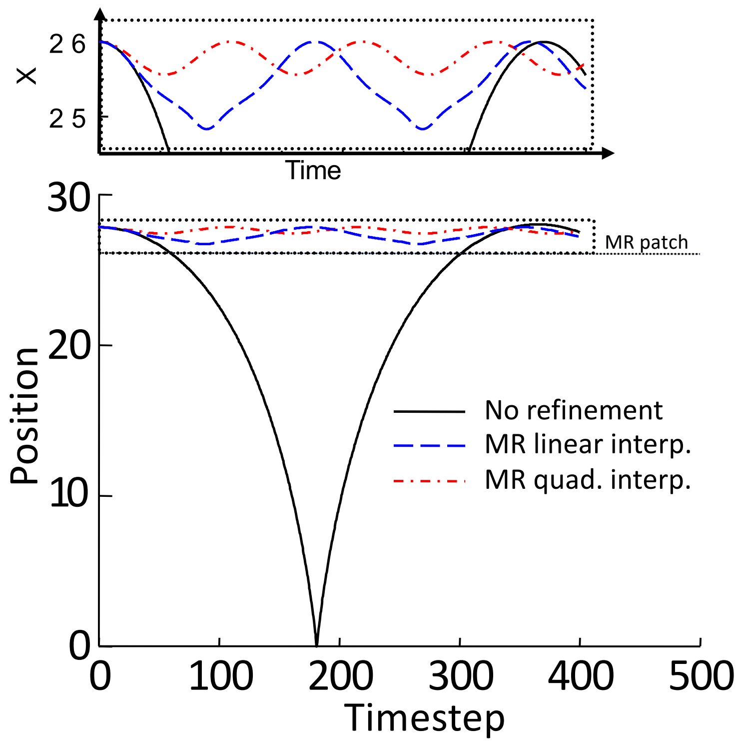

Spurious self-force: magnitude map

Map of spurious self-force as a function of particle position in refinement patch

32x32 refinement patch

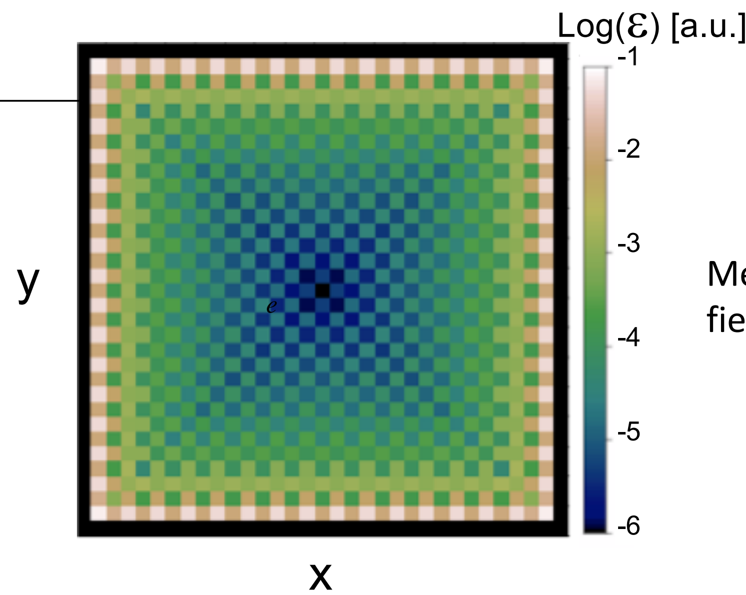

$$\varepsilon = \sqrt{(E_x - E_x^{\mathrm{ref}})^2 + (E_y - E_y^{\mathrm{ref}})^2}$$

Mesh refinement field

Physical field

Spurious self-force decreases rapidly in patch

Spurious self-force: mitigation

Add buffer region surrounding refined area

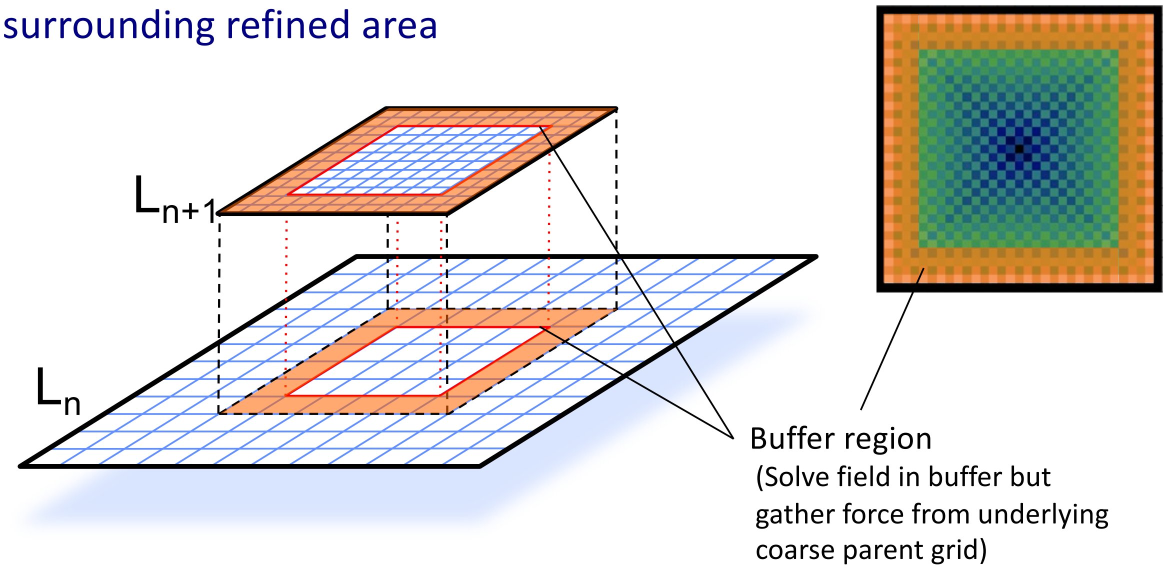

1 – solve on coarse grid,
2 – interpolate on fine grid boundaries,
3 – solve on fine grid,
4 – disregard fine grid solution close to edge when gathering force onto particles.

Thickness of buffer region provides user control of relative magnitude of spurious force.

Spurious self-force: mitigation

Test using script test1partin1patch.py:

- **Run with l_mr=1, ntransit=0.**

Example with 2 and 4
guard cells buffer region

No buffer: particle trapped in patch.

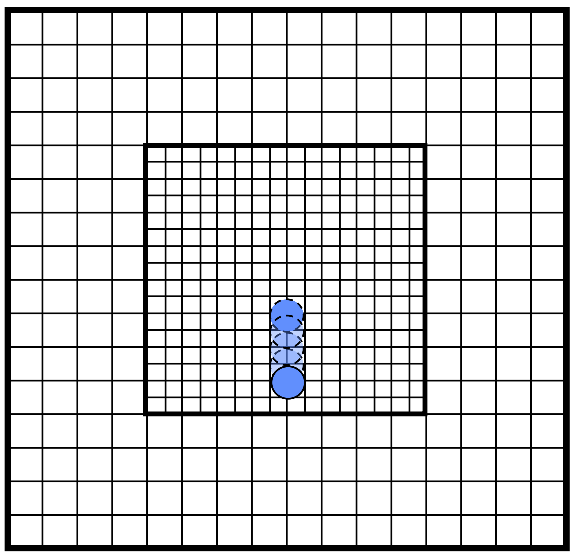

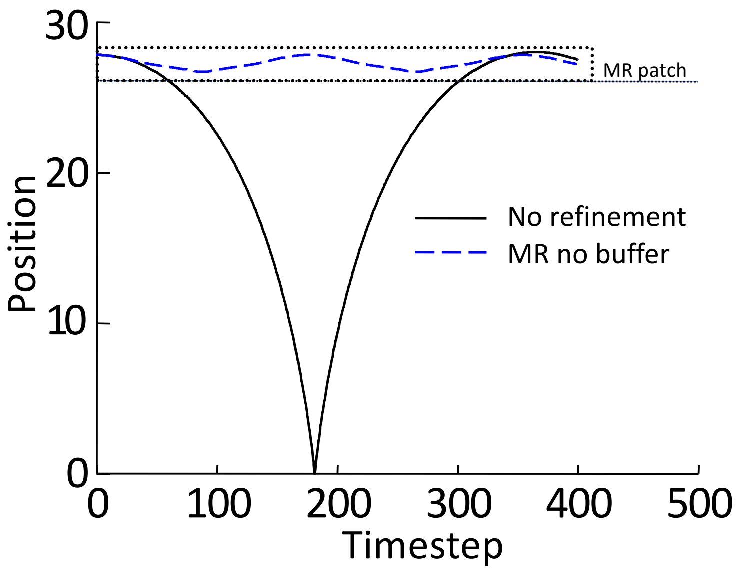

Spurious self-force: mitigation

Test using script test1partin1patch.py:

- **Run with l_mr=1, ntransit=1.**

Example with 2 and 4 guard cells buffer region

With buffer: no more trapping

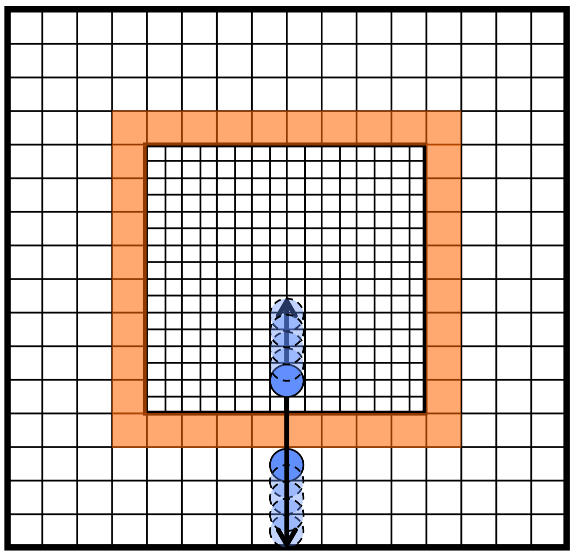

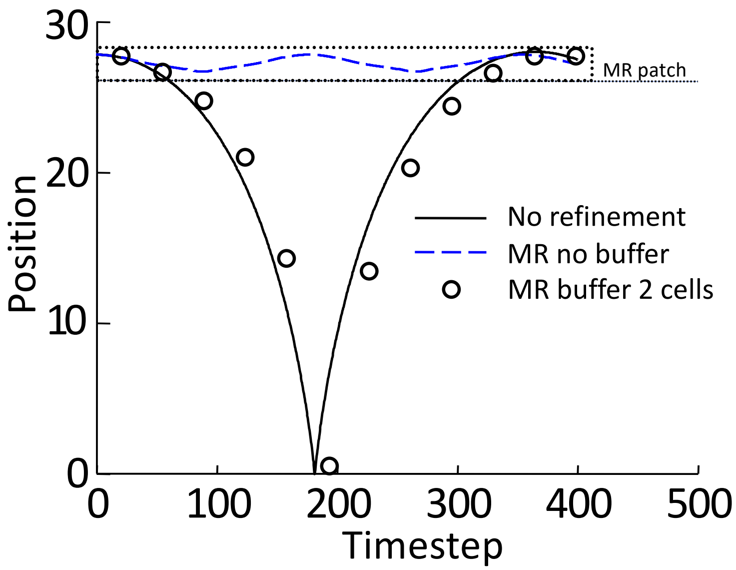

Spurious self-force: mitigation

Test using script test1partin1patch.py:

- **Run with l_mr=1, ntransit=2.**

Example with 2 and 4 guard cells buffer region

With buffer: no more trapping
4 guard cells better than 2

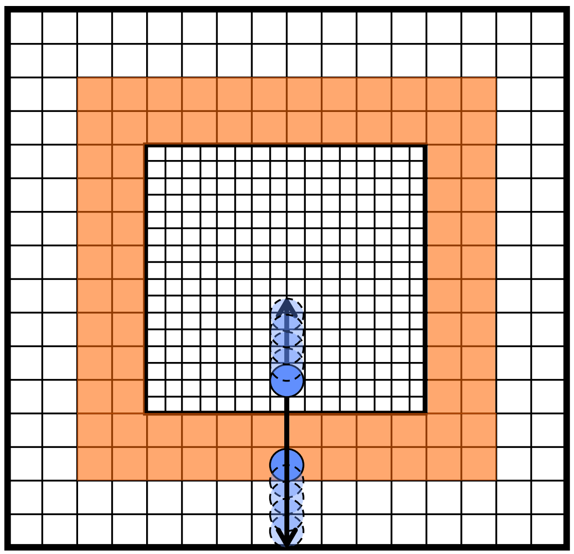

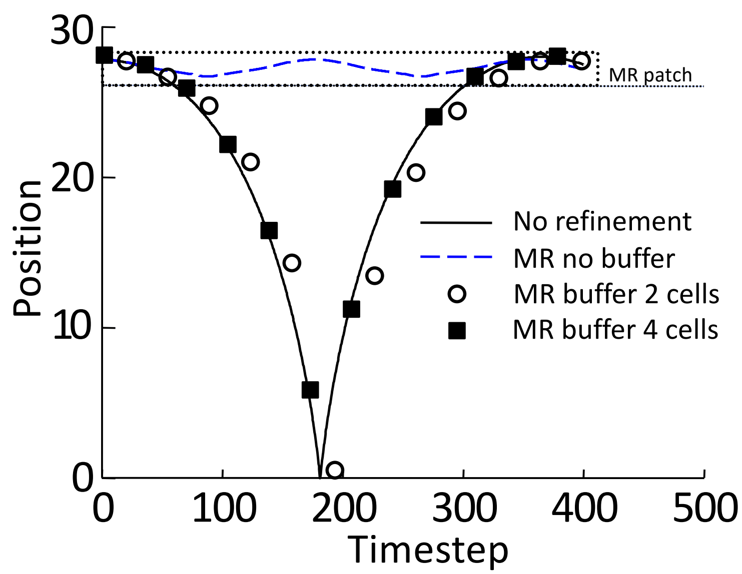

Buffer region is very effective.

Electrostatic AMR PIC example: HCX

High Current Experiment
(High Brightness Beam Transport Campaign, 2005)

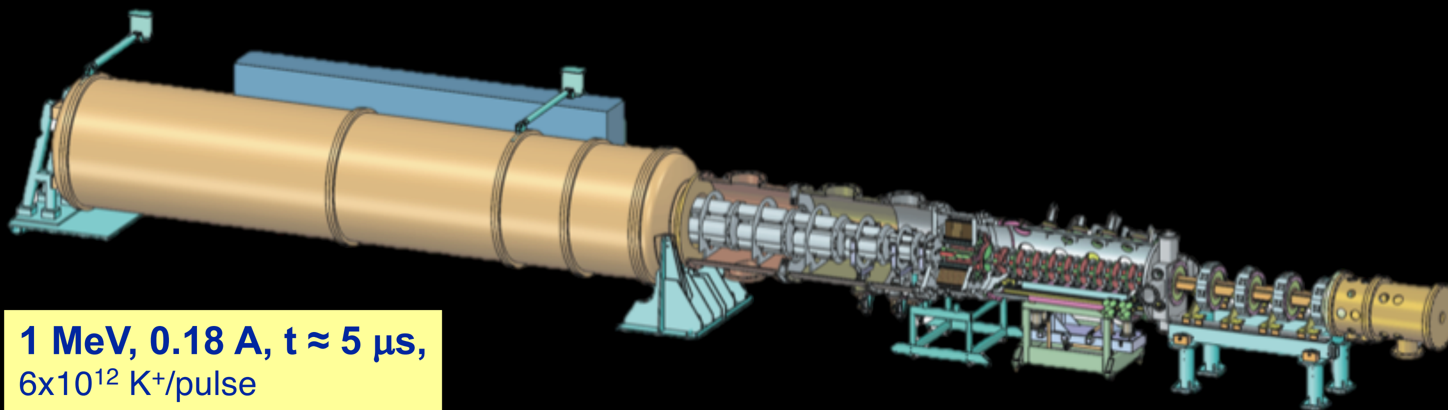

1 MeV, 0.18 A, t ≈ 5 μs,
6×10^{12} K^+/pulse

Heavy Ion Fusion program, LBNL

Electrostatic AMR PIC example: HCX

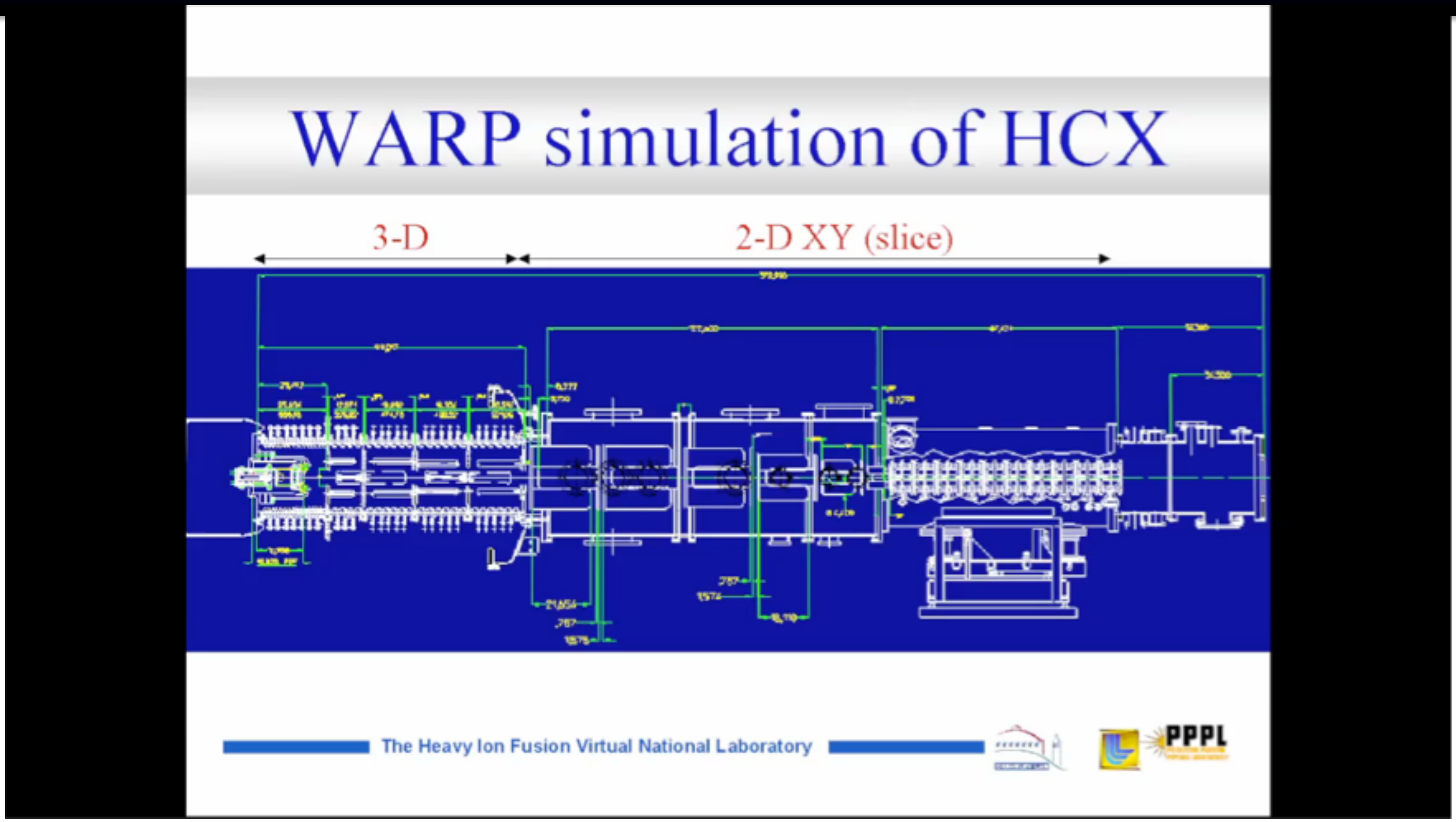

Electrostatic AMR PIC example: HCX

Very high resolution needed
to model the source.

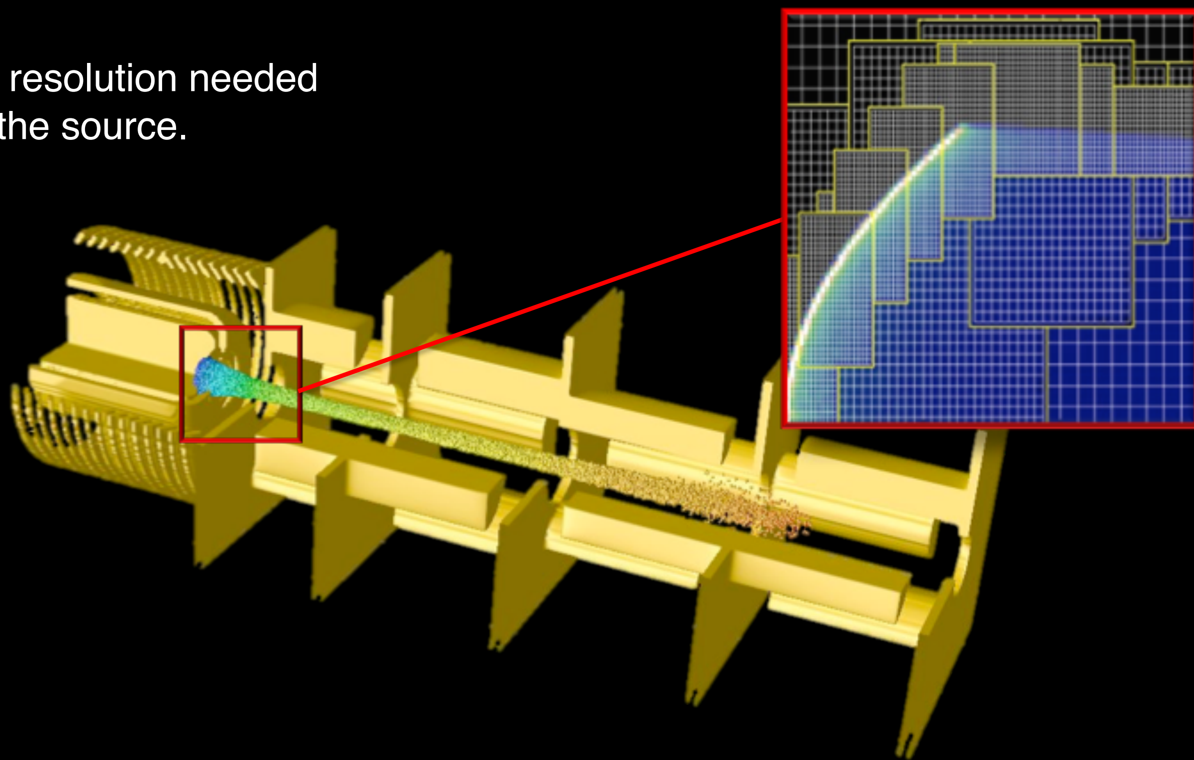

Source region is axisymmetric and is well captured with RZ simulations.

Modeling of source critical - determines initial shape of beam.

Axisymmetric (RZ) time-dependent simulations.

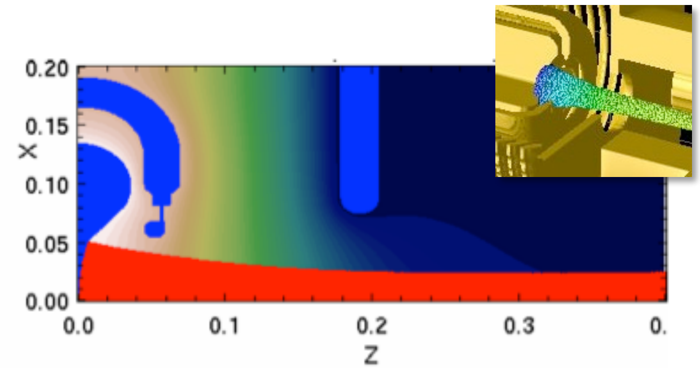

Run	Grid size	Nb particles
Low res.	56x640	~1M
Medium res.	112x1280	~4M
High res.	224x2560	~16M
Very High res.	448x5120	~64M

A fairly high resolution is needed to reach convergence

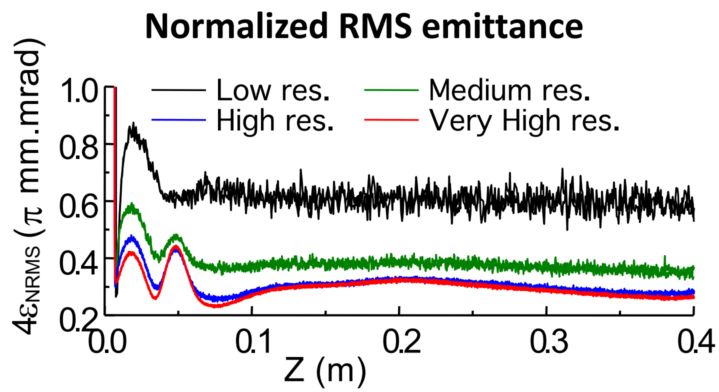

First MR attempt - 1 MR block surrounding emitter.

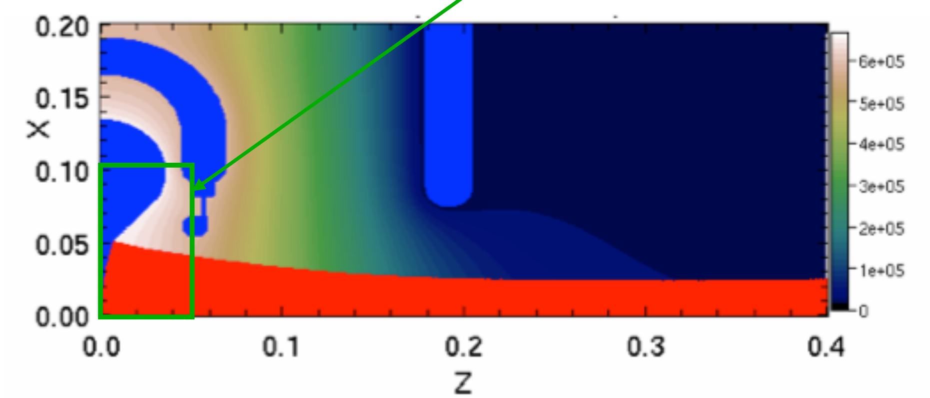

Refining around the emitter area is enough to recover emittance from converged high-resolution case.

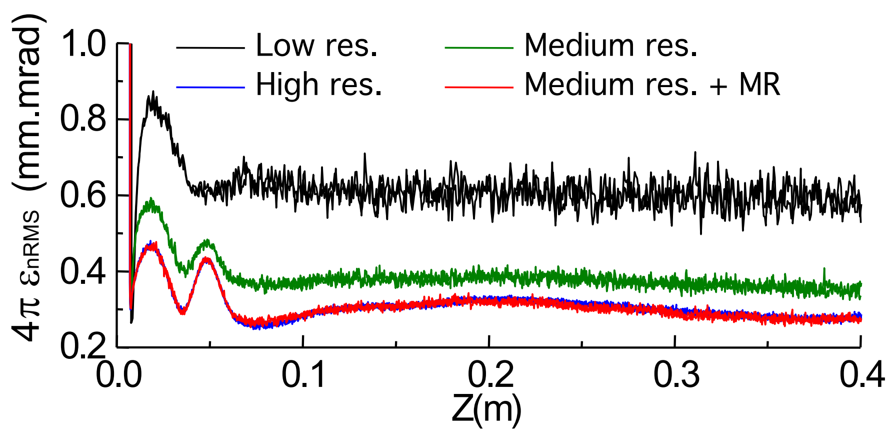

Run	Grid size	Nb particles
Low res.	56x640	~1M
Medium res.	112x1280	~4M
High res.	224x2560	~16M
Medium res. + MR	112x1280	~4M

First MR attempt - 1 MR block surrounding emitter (2).

However, it is not enough for recovering details of distribution.

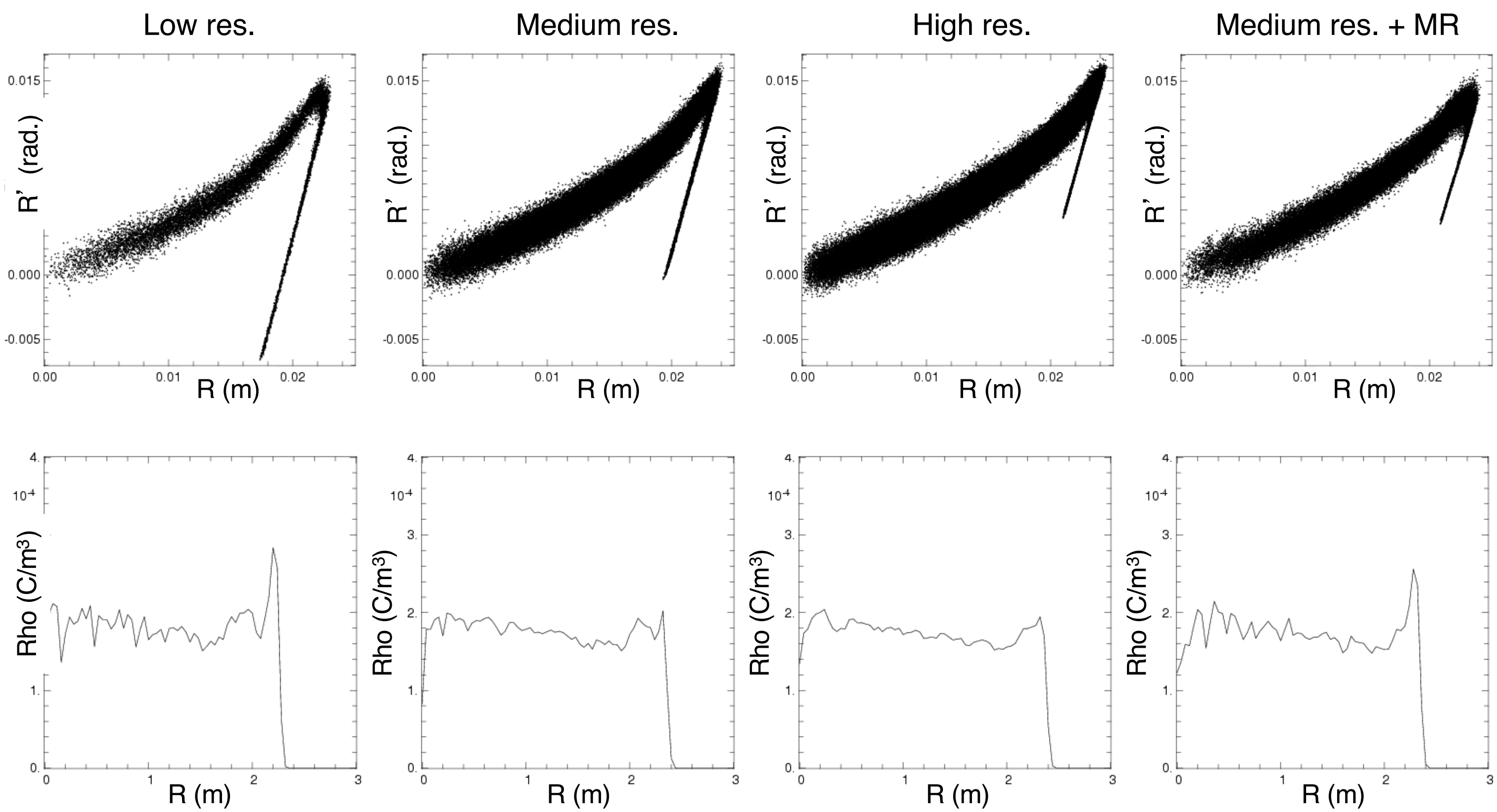

(plots from data at z=0.4m)

Full adaptive mesh refinement implementation
--speedup from AMR: x10

Run	Grid size	Nb particles
Low res.	56 x 640	~1M
Medium res.	112 x 1280	~4M
High res.	224 x 2560	~16M
Low res. + AMR	56 x 640	~1M

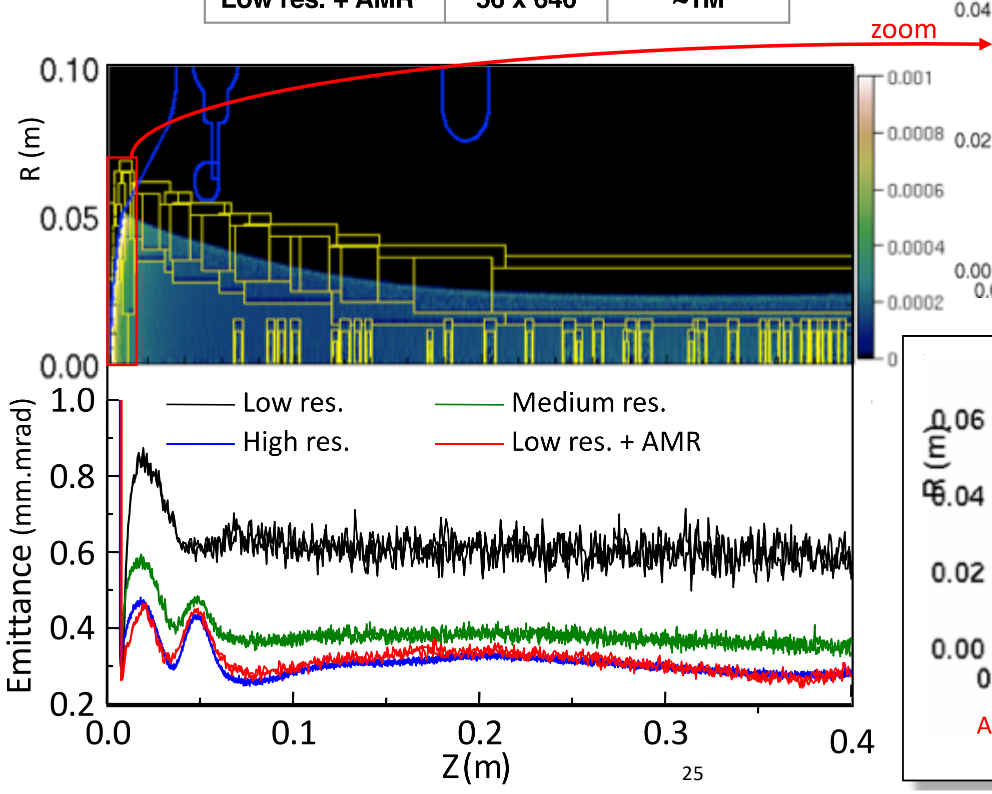

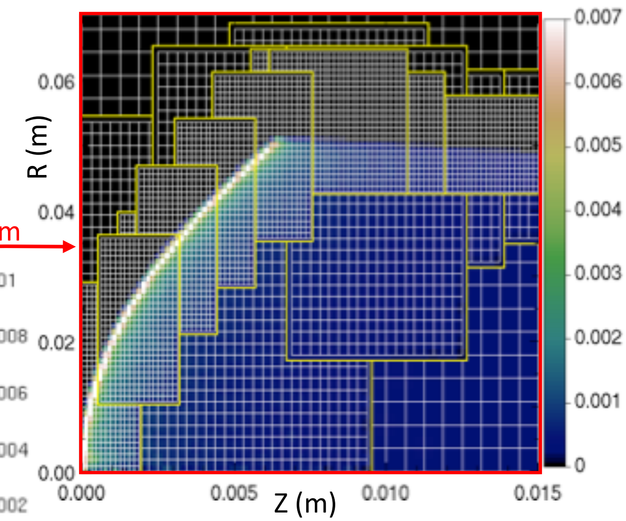

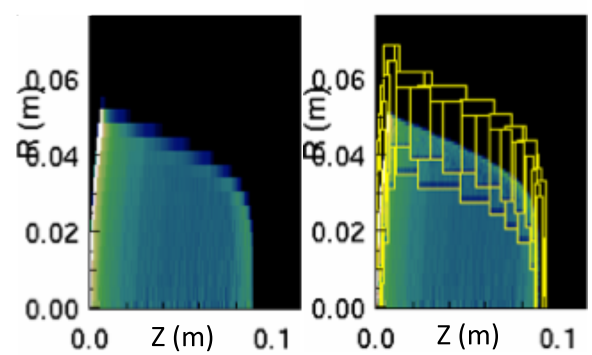

Automatic mesh refinement follows gradients: emitting area, beam edge and front.

25

Full adaptive mesh refinement implementation

--speedup from AMR: x10

Full AMR enable recovery of details of distribution.

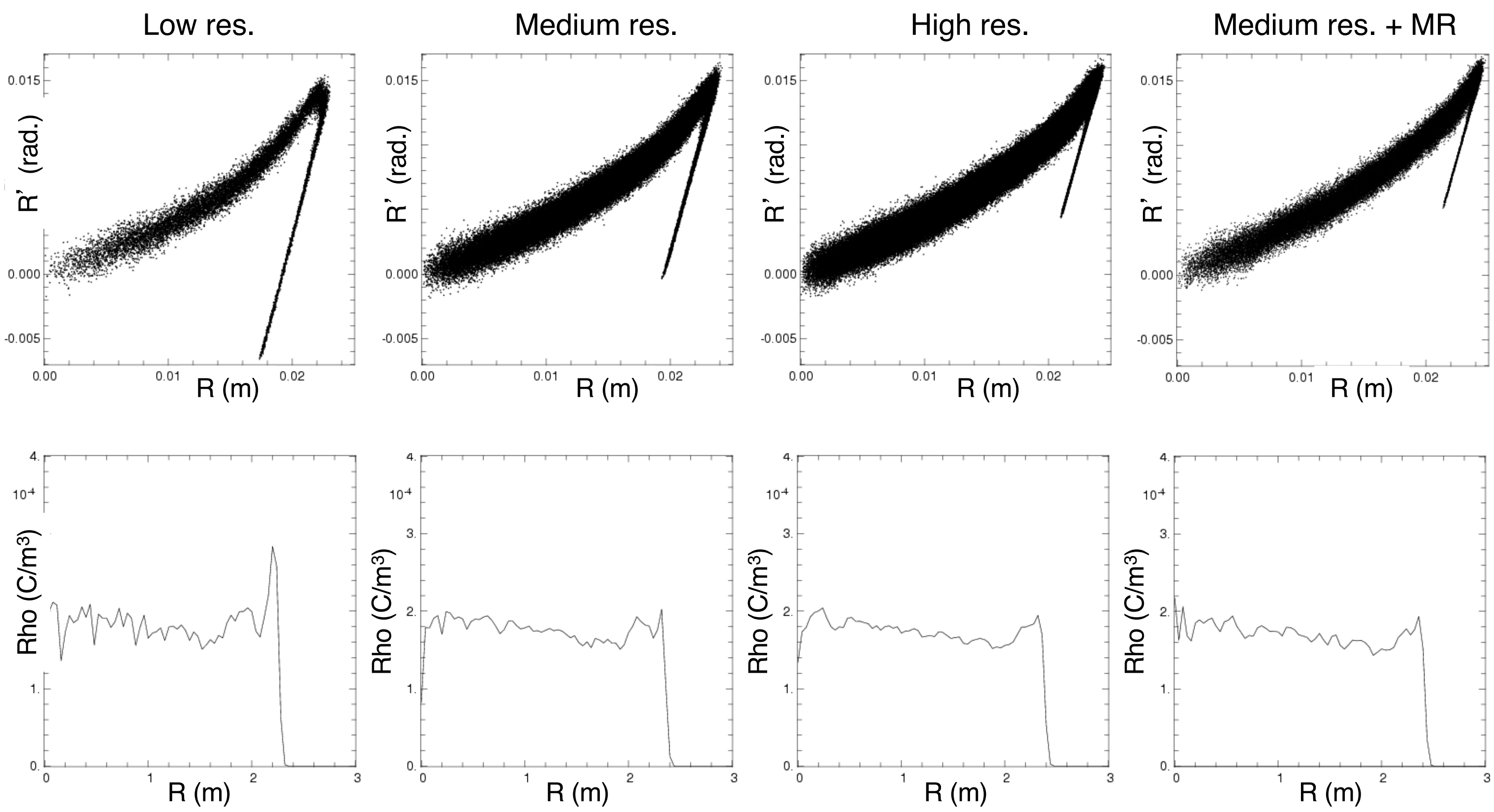

(plots from data at z=0.4m)

Example of AMR at edge of beam

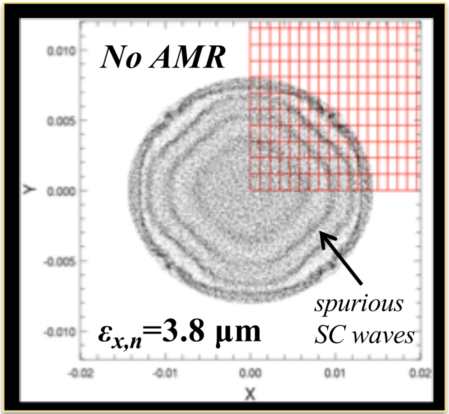

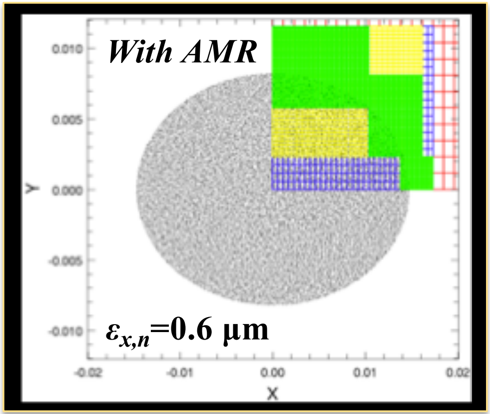

Test using script testxy_amr.py:

- **Run with case='lowres', then 'highres' and 'AMR'.**
- **Observe how using AMR enables accurate simulation at reduced CPU cost.**

Summary of electrostatic AMR-PIC

- Simple method for electrostatic AMR-PIC was presented.
- Buffer region mitigates spurious self-force effect very effectively.
- Speedups of x10 demonstrated on simulation of injector.
- Alternate methods such as multipole expansions have other advantages & drawbacks.

Outline

- Why mesh refinement?
- Potential issues
- Electrostatic mesh refinement
  - spurious self-force example
  - spurious self-force mitigation
  - application to the modeling of HCX injector
- <u>Electromagnetic mesh refinement</u>
  - spurious reflection of waves
  - spurious reflection of waves mitigation
  - Application to the modeling beam-induced plasma wake
- Special mesh refinement for particle emission
- Summary

1-D FDTD EM wave equation

- We consider 1d wave equation (natural units)

$$\frac{\partial E}{\partial t} = \frac{\partial B}{\partial x}; \quad \frac{\partial B}{\partial t} = \frac{\partial E}{\partial x}$$

- staggered on a regular space time grid using finite-difference time-domain (FDTD) centered scheme

$$\frac{E_j^{i+1} - E_j^i}{\delta t} = \frac{B_{j+1/2}^{i+1/2} - B_{j-1/2}^{i+1/2}}{\delta x}$$

$$\frac{B_{j+1/2}^{i+1/2} - B_{j+1/2}^{i-1/2}}{\delta t} = \frac{E_{j+1}^i - E_j^i}{\delta x}$$

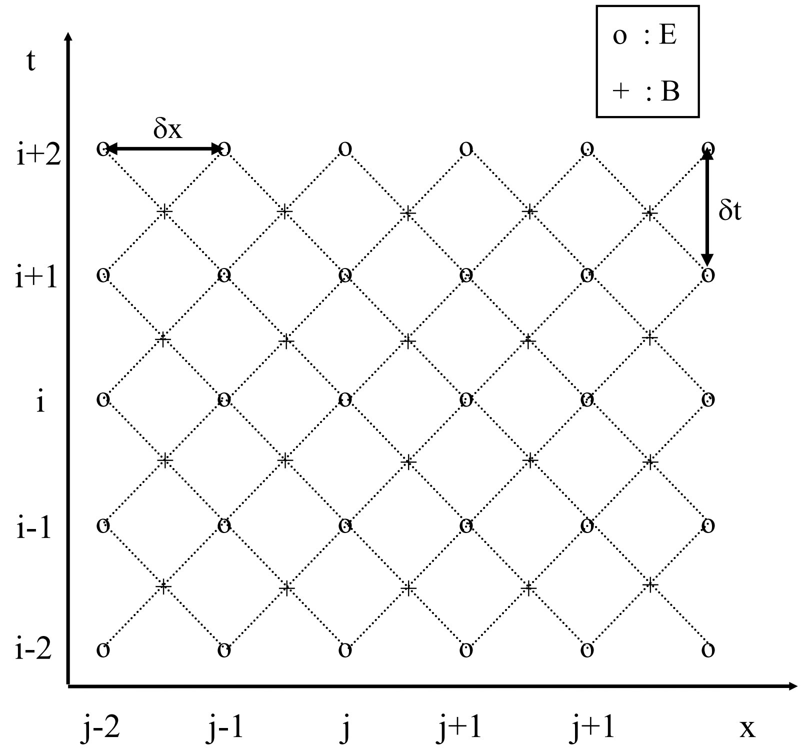

1-D MR-EM: space refinement
uncentered finite-difference

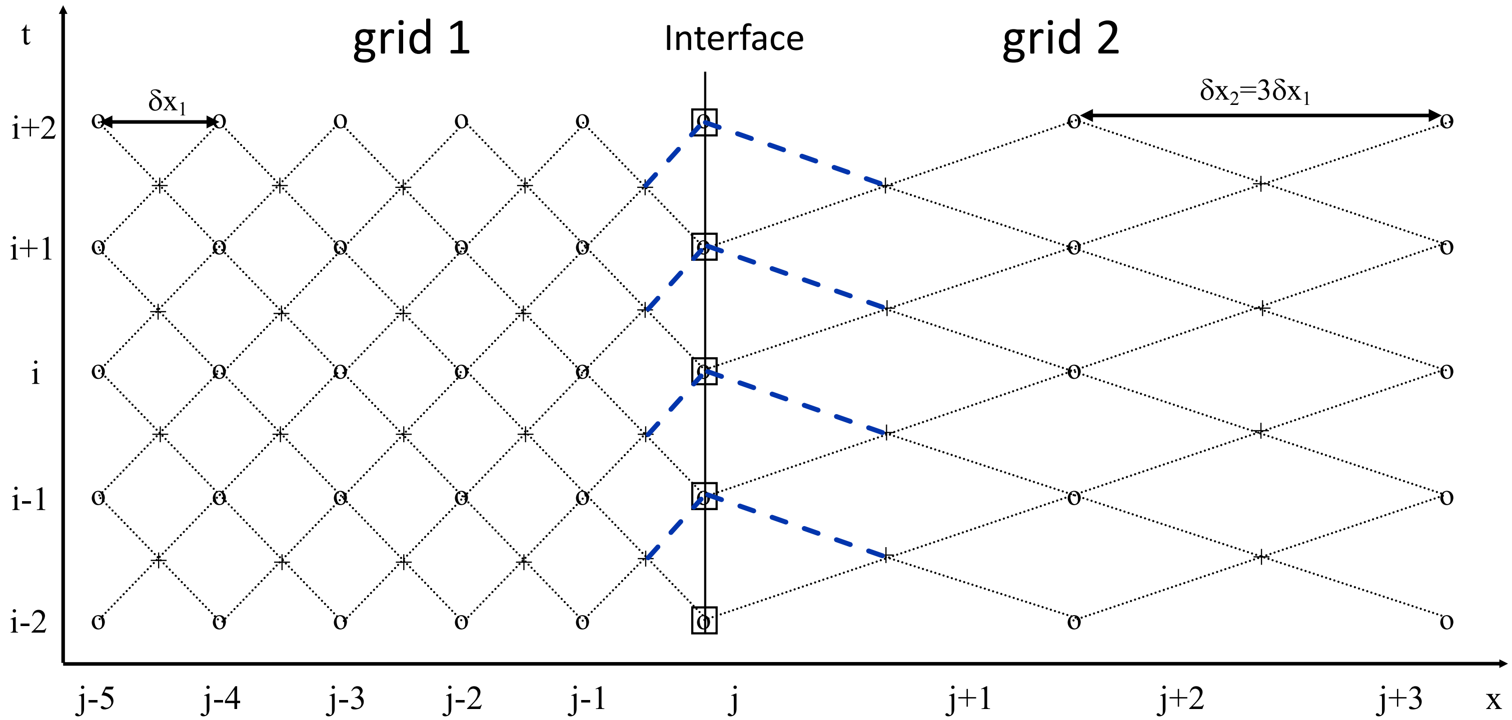

o, + : finite-difference at positions ≠j

$\boxed{o}$: finite-volume (=uncentered FD) at j

$$\frac{E_j^{i+1}-E_j^i}{\delta t}=2\frac{B_{j+1/2}^{i+1/2}-B_{j-1/2}^{i+1/2}}{\delta x_1+\delta x_2} \quad \text{(method 1)}$$

or

$$\frac{E_j^{i+1}-E_j^i}{\delta t}=\frac{B_{j+1/2}^{i+1/2}}{\delta x_2}-\frac{B_{j-1/2}^{i+1/2}}{\delta x_1} \quad \text{(method 2)}$$

1-D MR-EM: space refinement

centered finite-difference

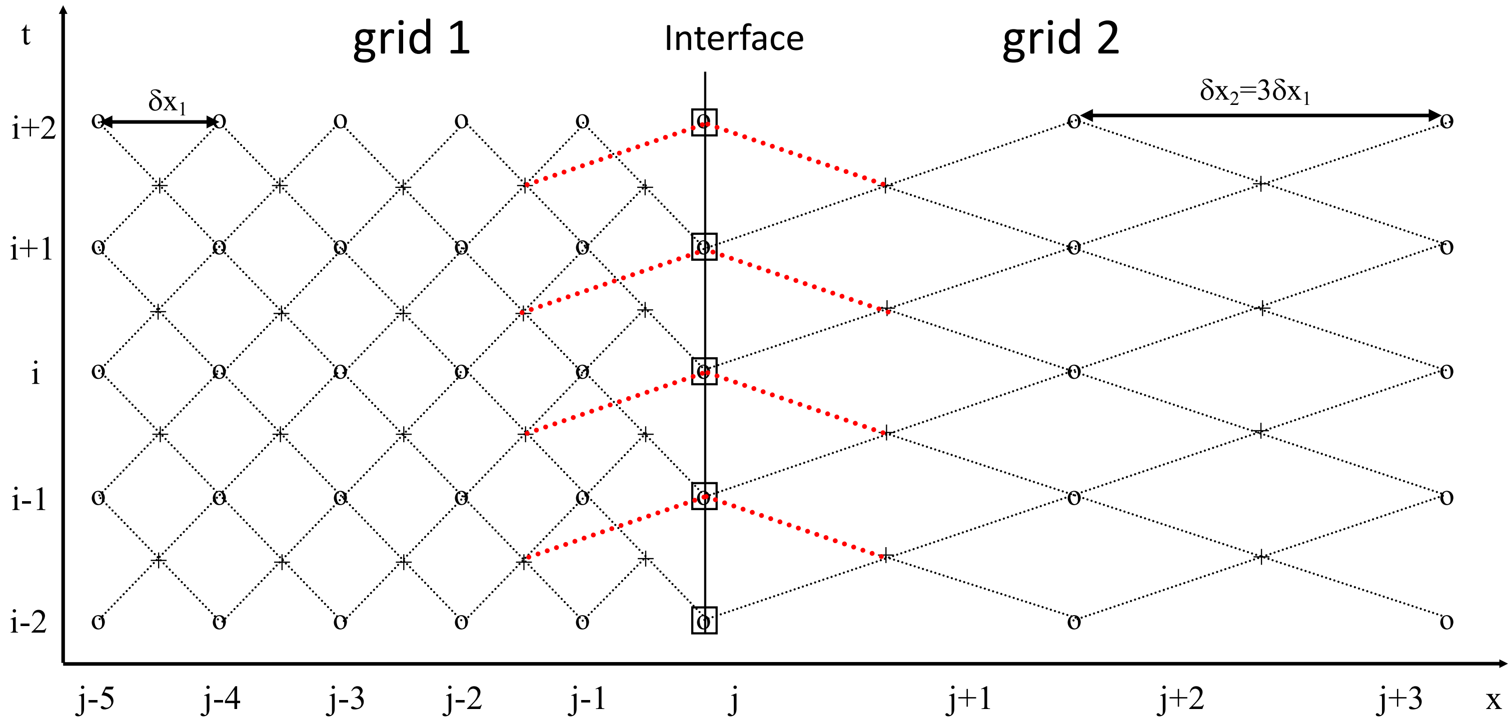

o, + : finite-difference at positions ≠j

o : ‘jump’ inside fine grid at j

$$\frac{E_j^{i+1} - E_j^i}{\delta t} = \frac{B_{j+1/2}^{i+1/2} - B_{j-n/2}^{i+1/2}}{\delta x_2}$$ (method 3)

1-D MR-EM: coefficients of spurious reflection

Test to measure spurious reflection R at interface at j of signal injected on fine grid.

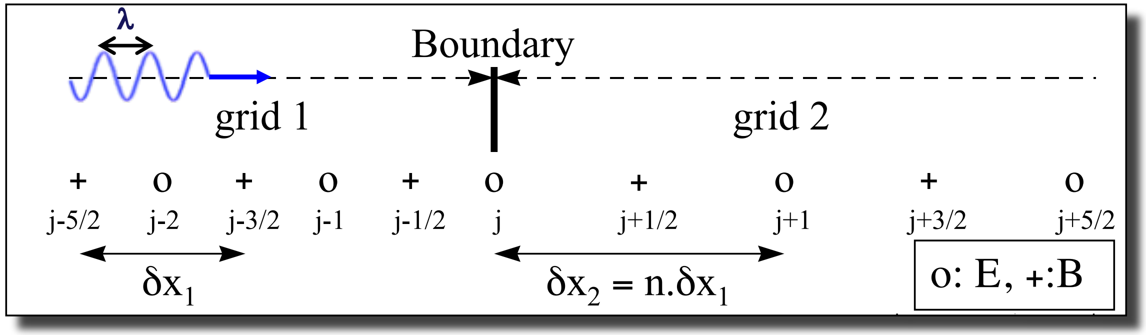

Reflection

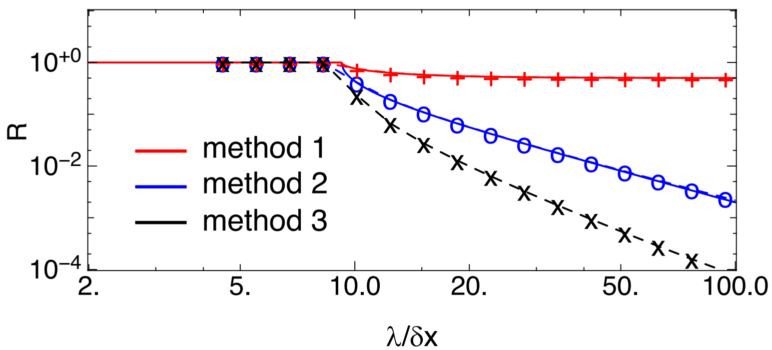

Total energy

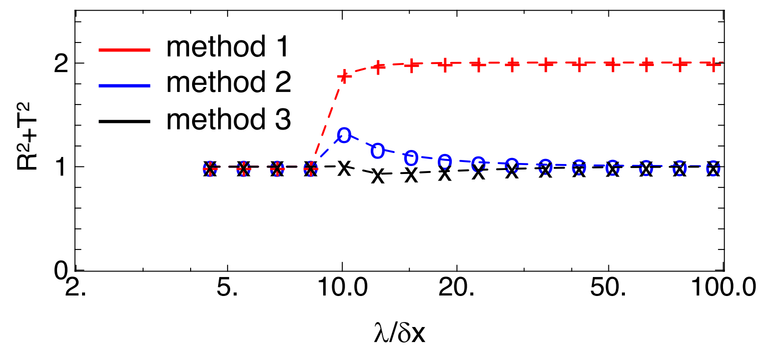

$\lambda \leq \lambda_{Nyquist}$ of coarse grid are reflected with amplification of total energy!

Warp & WarpX's Electromagnetic MR use PML and substitution to prevent reflections

- Termination of patches with Perfectly Matched Layers (PML) to avoid spurious reflections
- Buffer zone used for mitigating spurious self-force

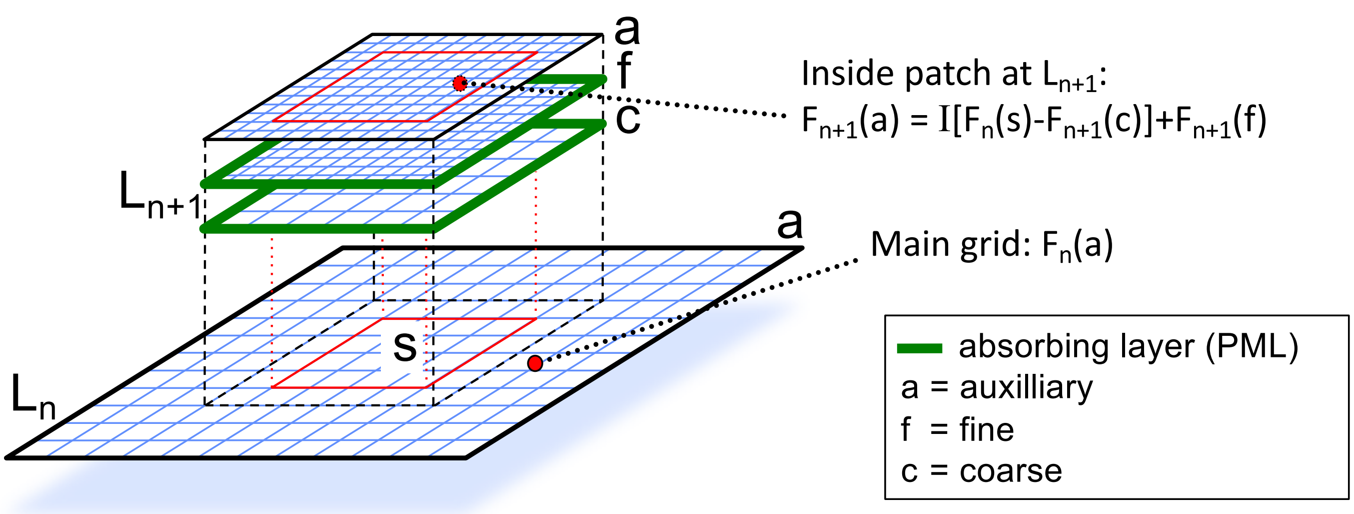

MR procedure is recursive, accommodating an arbitrary number of levels

Example with two levels of refinement

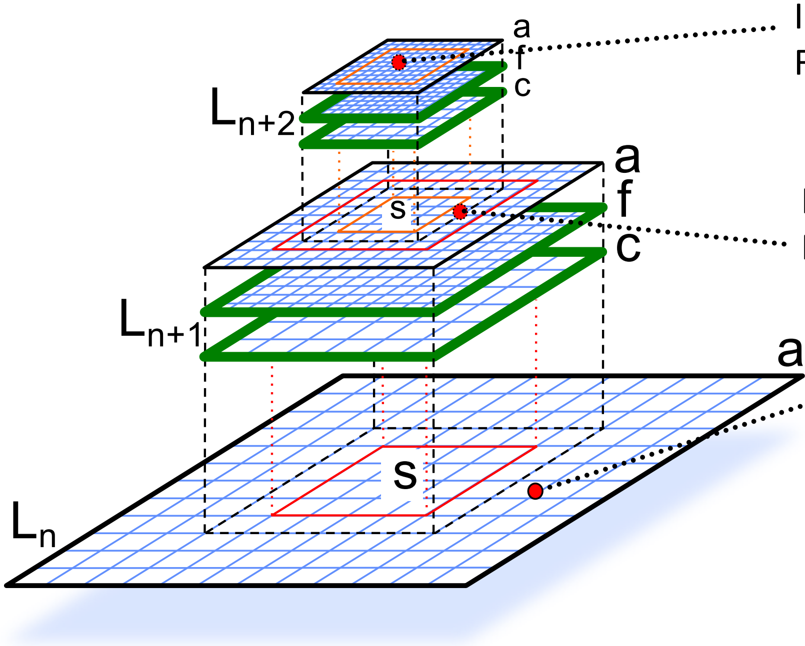

Inside patch at L_{n+2}:
$F_{n+2}(a) = I[F_{n+1}(s)-F_{n+2}(c)]+F_{n+2}(f)$

Inside patch at L_{n+1}:
$F_{n+1}(a) = I[F_n(s)-F_{n+1}(c)]+F_{n+1}(f)$

Main grid: $F_n(a)$

absorbing layer (PML)
a = auxilliary
f = fine
c = coarse

Test with single particle

WarpX

Single particle orbiting around an external magnetic field, emitting synchrotron radiation

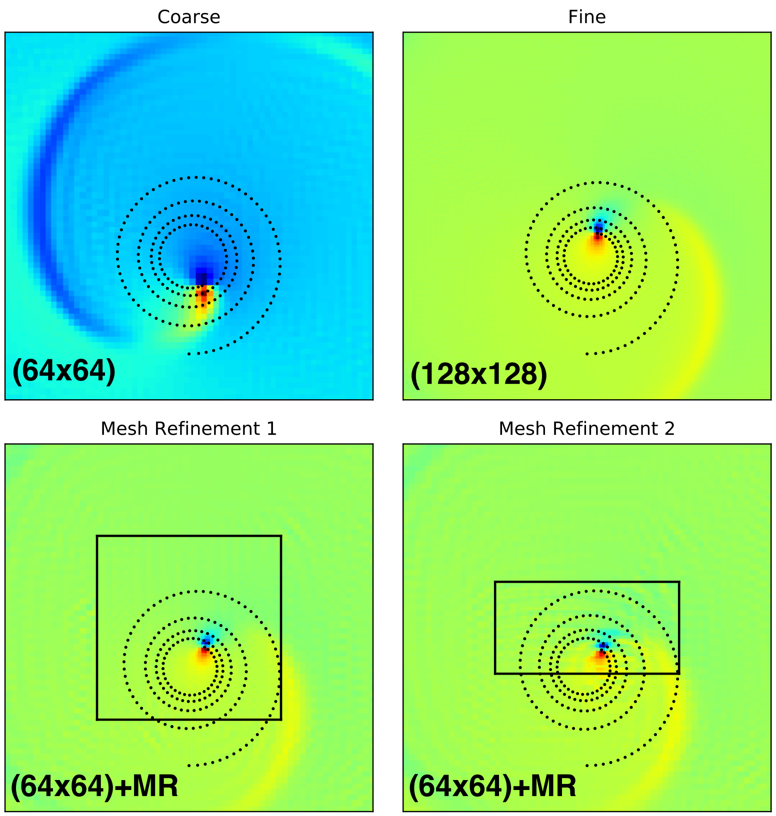

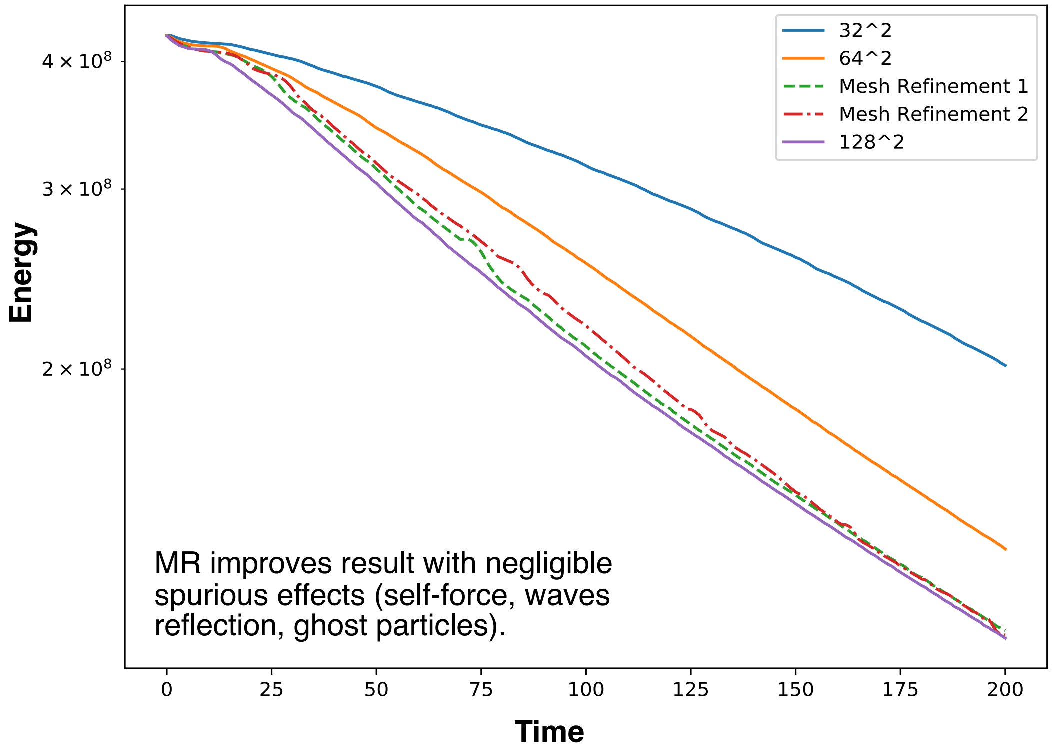

Note: buffer region not implemented yet; expected to improve results once implemented.

Validation on charged particle beam breathing

WarpX

Electron Gaussian distribution with inward initial radial velocity on top of static proton dist.

Electron beam contraction/expansion depends on resolution.

MR enables higher accuracy, covering fraction of box.

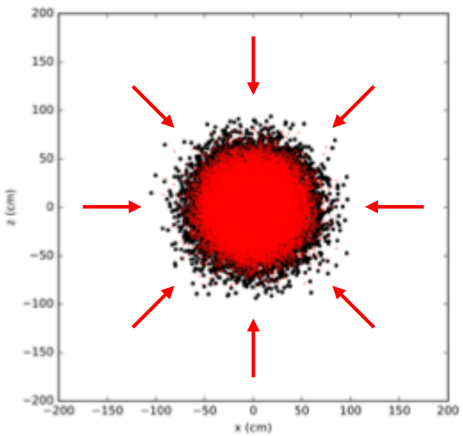

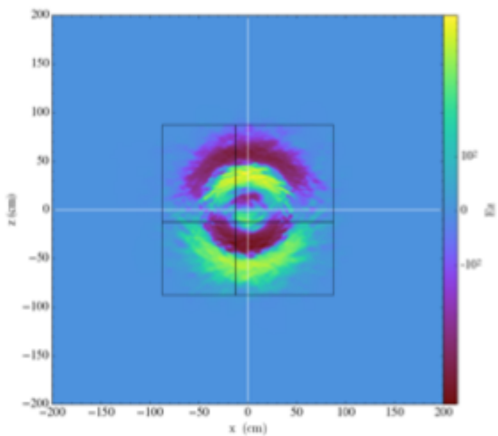

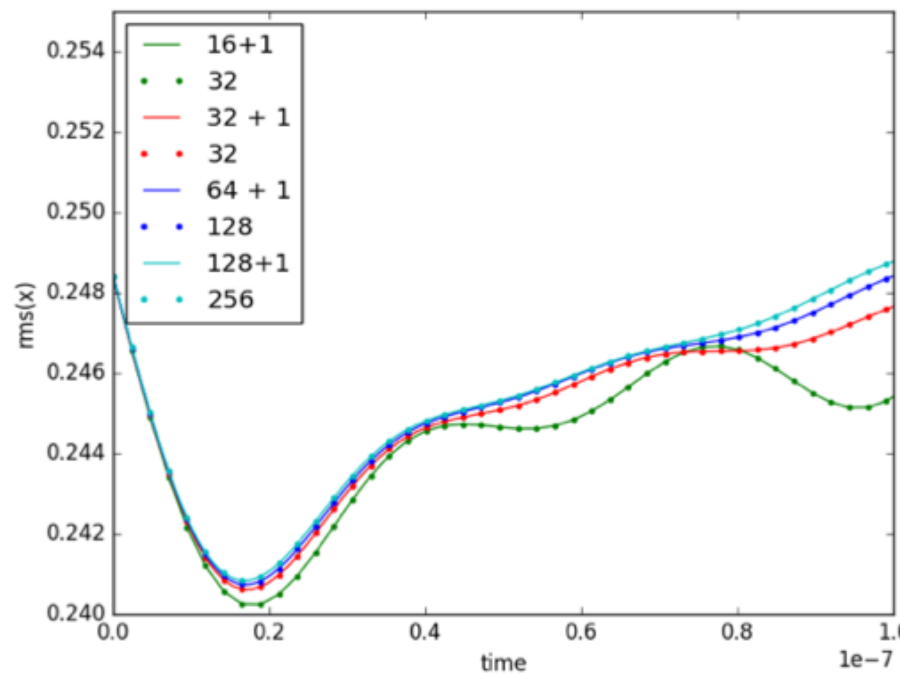

Laser injection with mesh refinement test

WarpX

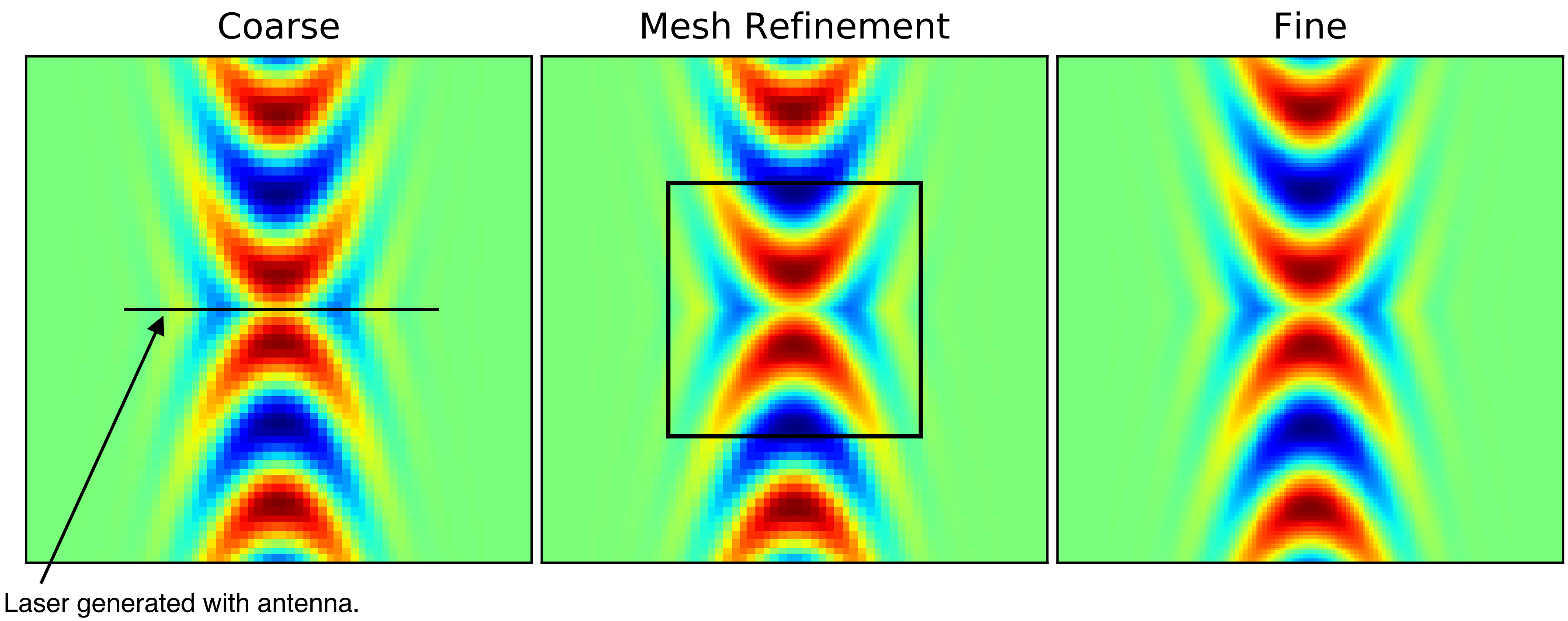

Example: simulation of beam-induced plasma wake

Warp

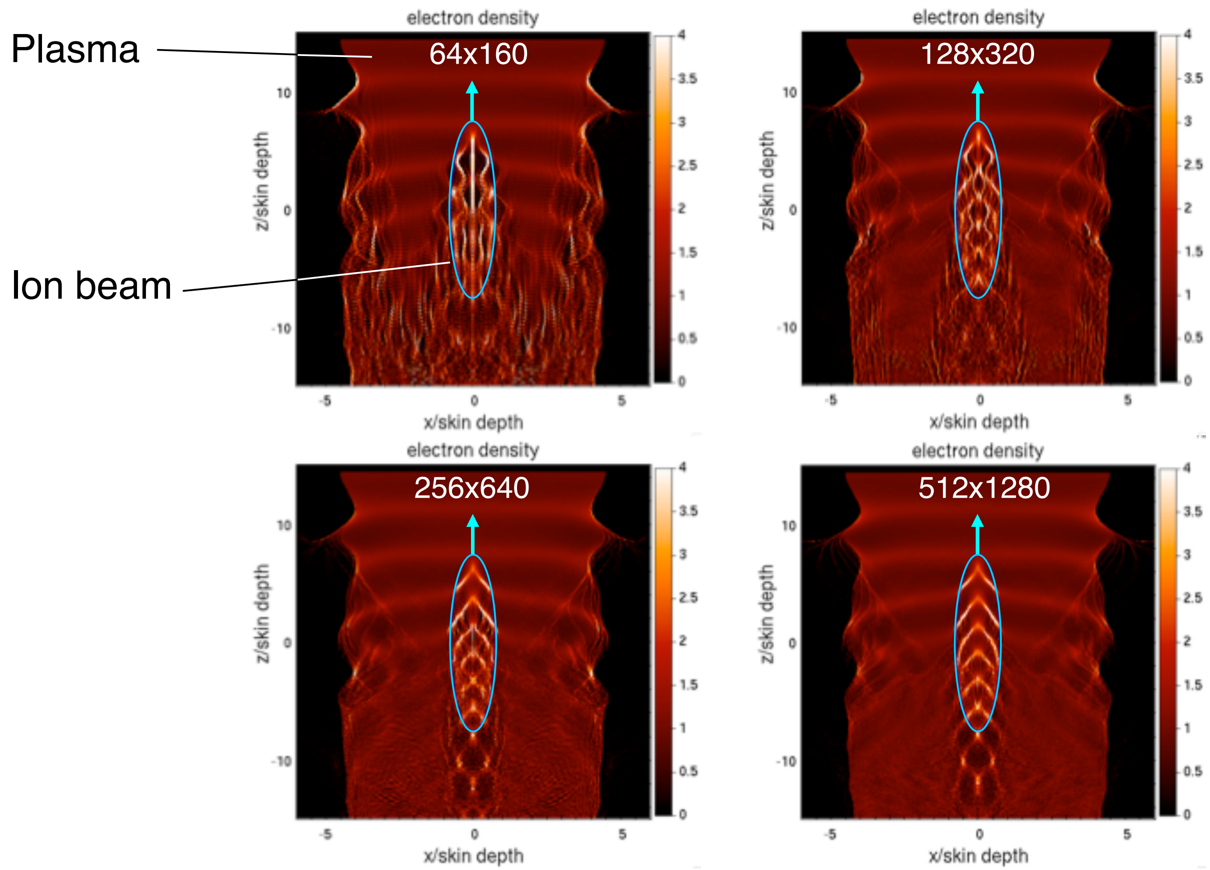

Slab XZ simulations

High resolution is needed to capture details.

Example: simulation of beam-induced plasma wake

Warp

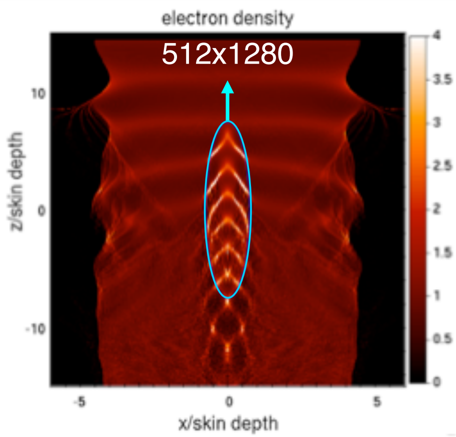

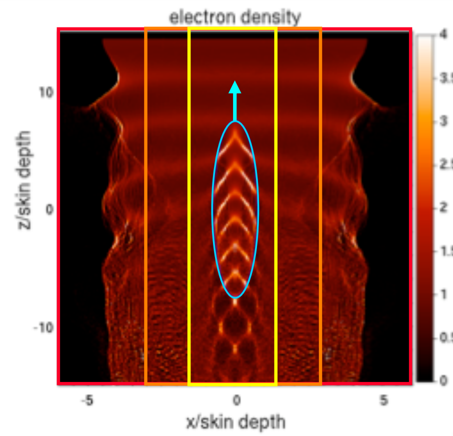

Mesh ref.
- 2 levels
- fields only

low resolution + MR
- 2 levels
- fields+ particles

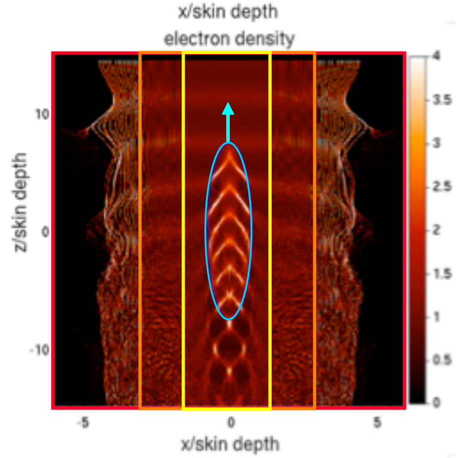

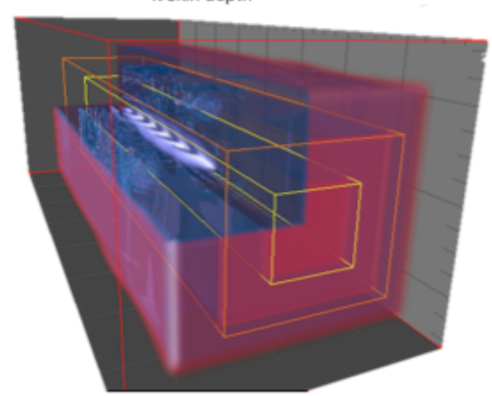

3-D

Speedup x10 in 3D (using the same time steps for all refinement levels).

First simulations of plasma accelerators with MR patch – 2-D

WarpX

Laser driven **2-D** **Particle beam driven**

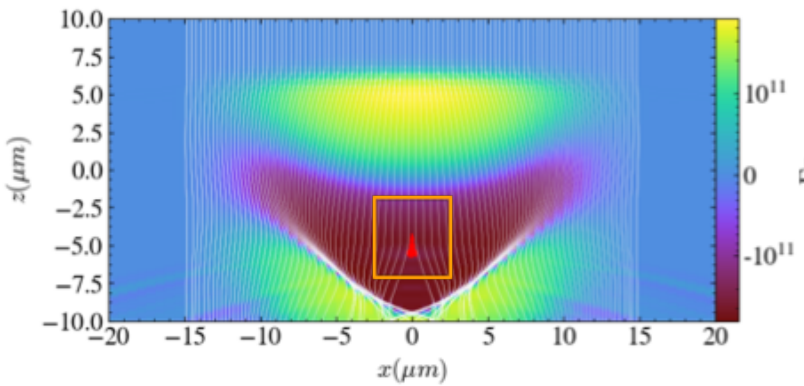

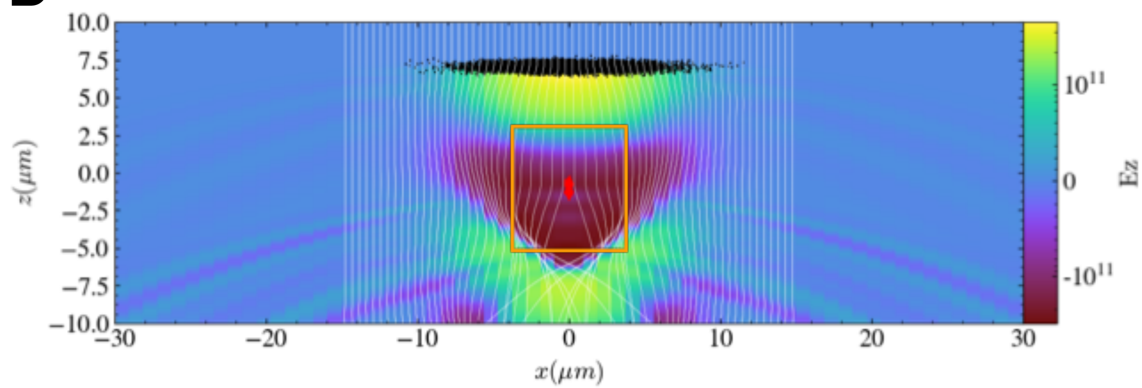

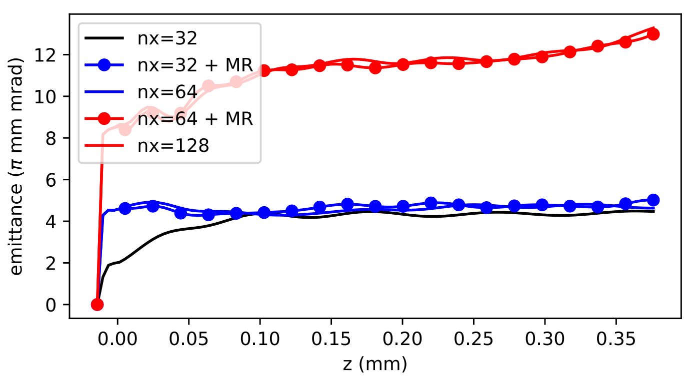

Simulations with small MR patch recover results using finer grid over the entire box.

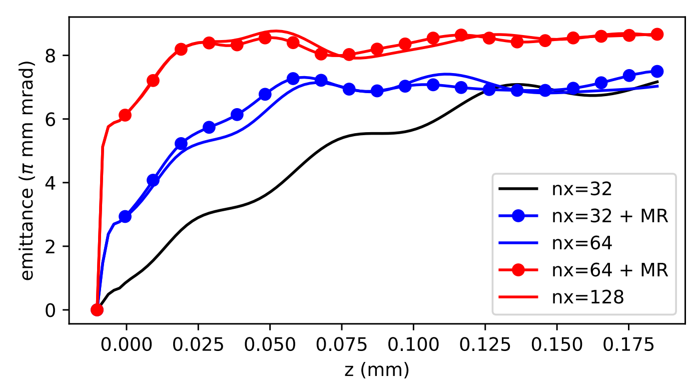

First simulations of plasma accelerators with MR patch – 3-D

WarpX

3-D

Laser driven

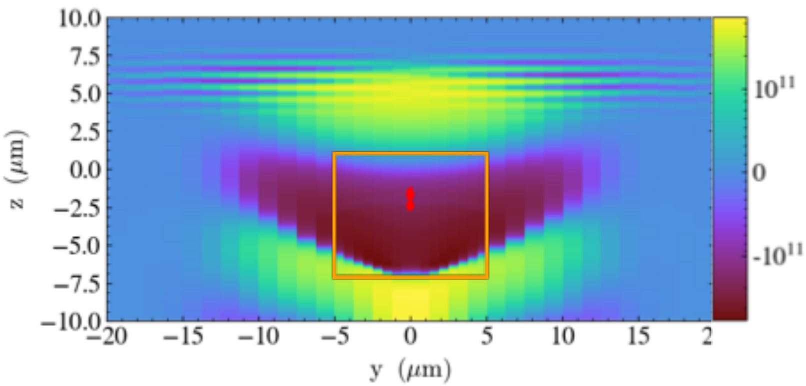

Particle beam driven

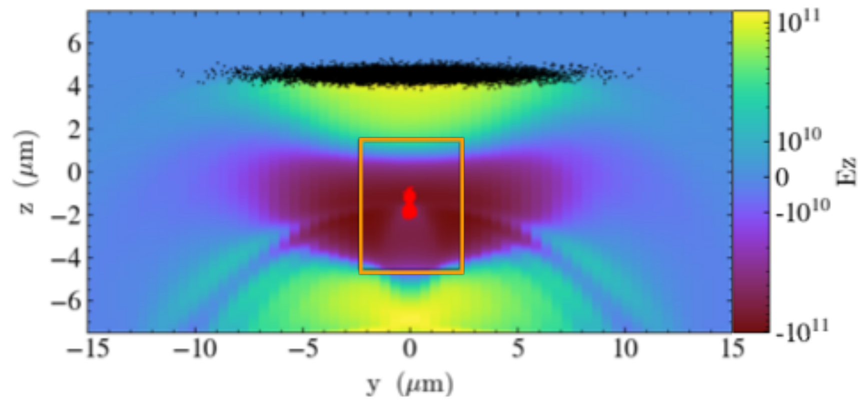

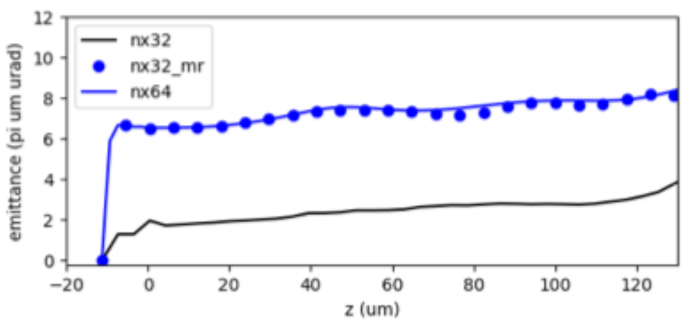

Simulations with small MR patch recover results using finer grid over the entire box.

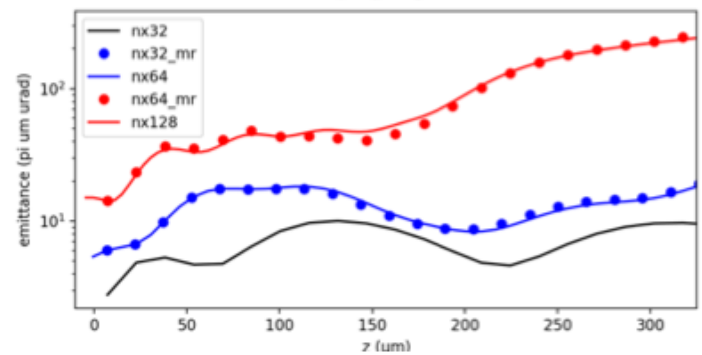

Movies of 3D runs

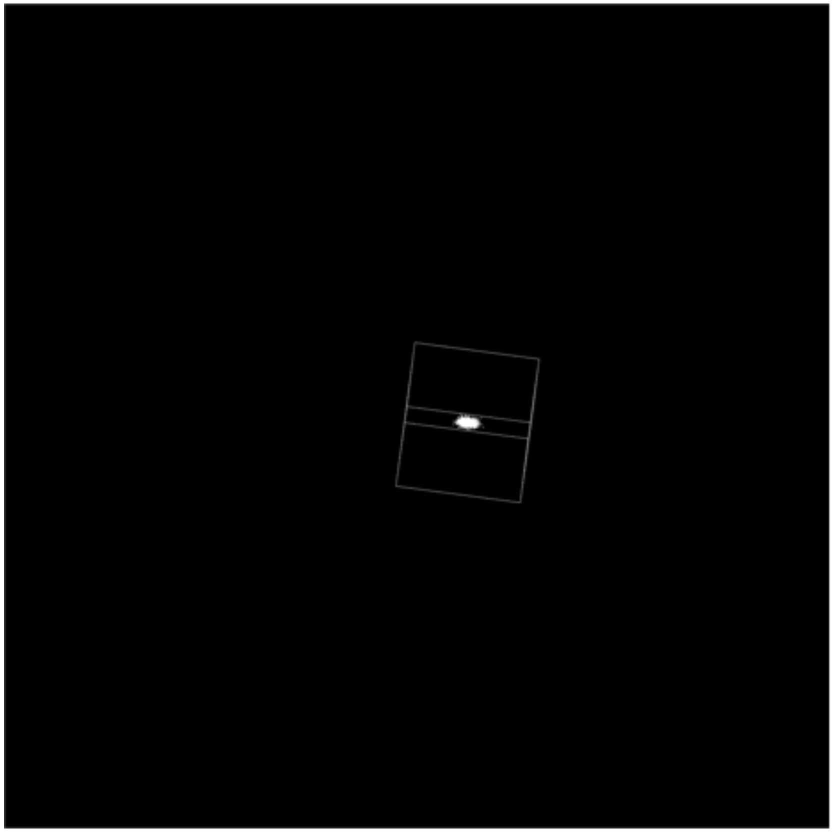

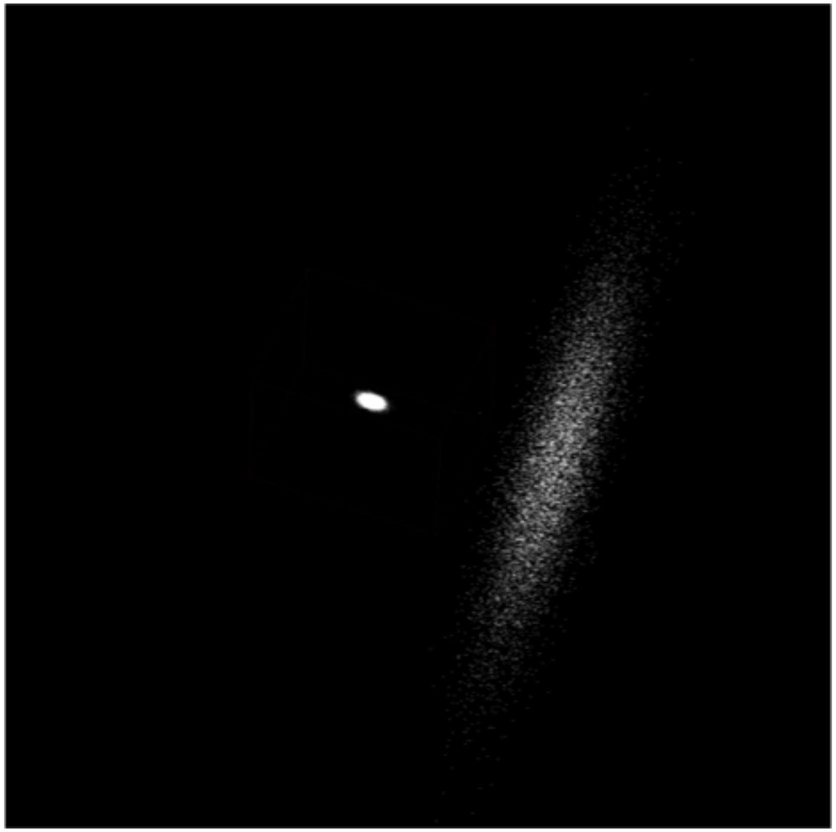

Movies by Maxence Thevenet

Outline

- Why mesh refinement?
- Potential issues
- Electrostatic mesh refinement
  - spurious self-force example
  - spurious self-force mitigation
  - application to the modeling of HCX injector
- Electromagnetic mesh refinement
  - spurious reflection of waves
  - spurious reflection of waves mitigation
  - Application to the modeling beam-induced plasma wake
- Special mesh refinement for particle emission
- Summary

44

3-D WARP simulation of HCX showed beam head scrapping

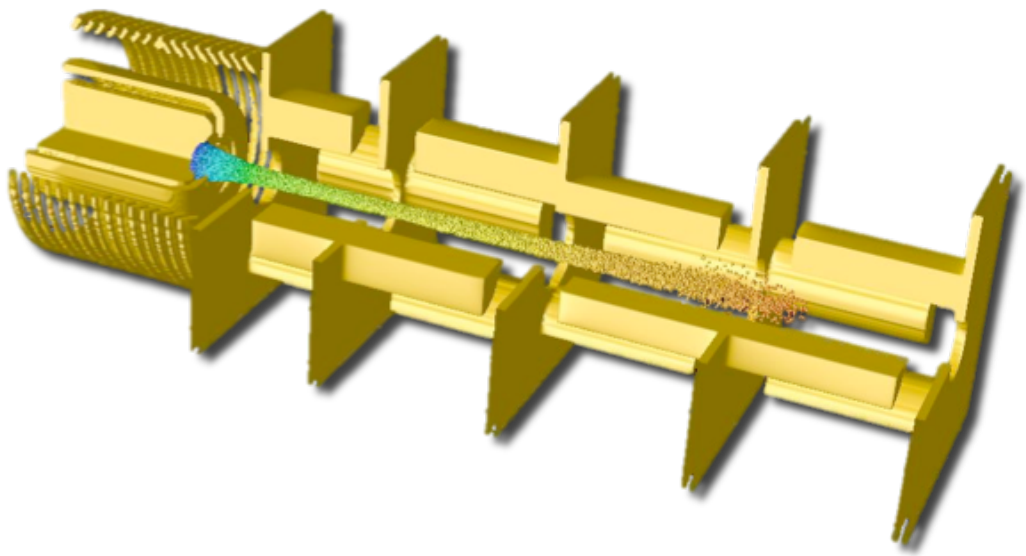

beam head particle loss < 0.1%

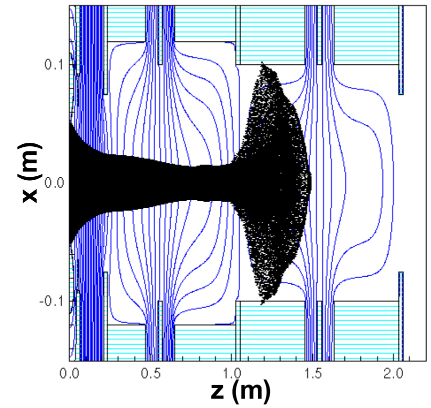

Rise-time τ = 400 ns

zero beam head particle loss

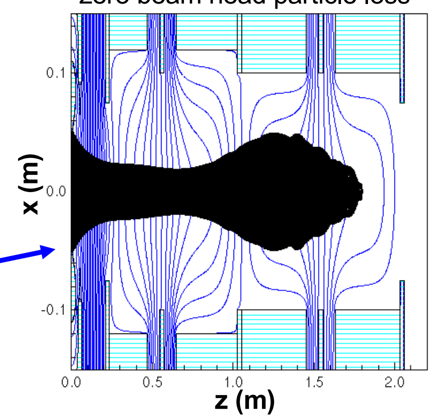

- Head cleaner with shorter voltage rise-time.
- Questions:
  - what is the optimal rise-time?
  - can we produce and model very-fast rise-time?

Test: 1-D time-dependent modeling of ion diode

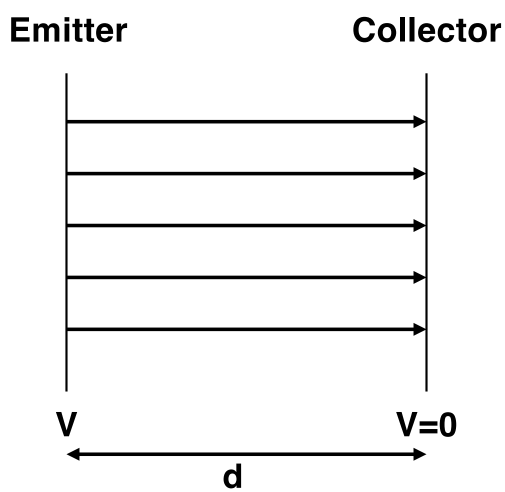

Applied voltage for Heavyside current history?

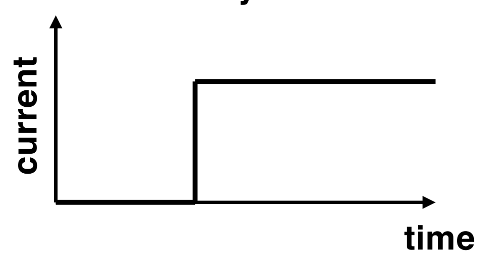

Analytic solution from Lampel-Tiefenback

$$V(t) = \frac{t}{3\tau}\left[4 - \left(\frac{t}{\tau}\right)^3\right] V_{\max}$$

(τ: transit time)

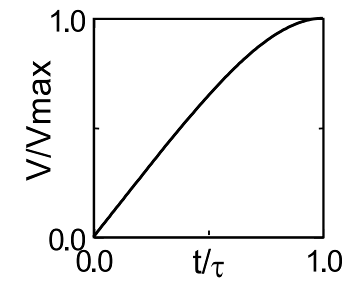

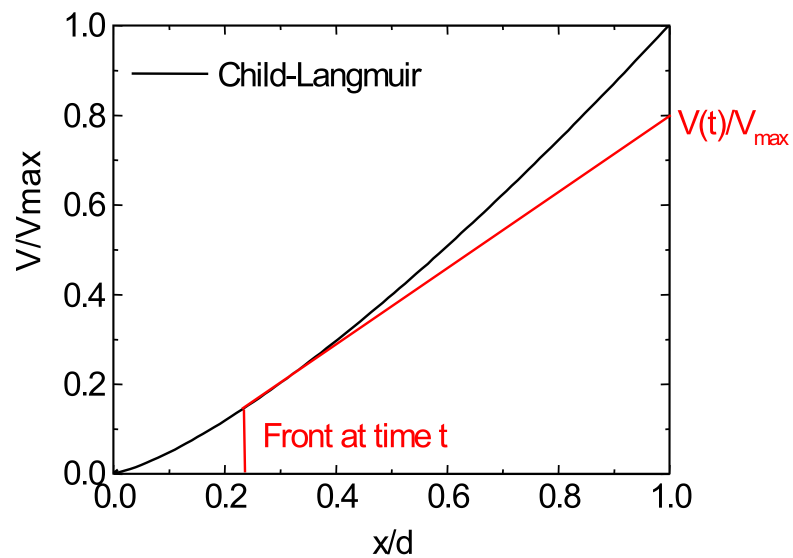

Test: 1D time-dependent modeling of ion diode (algo 1)

Injection algorithm

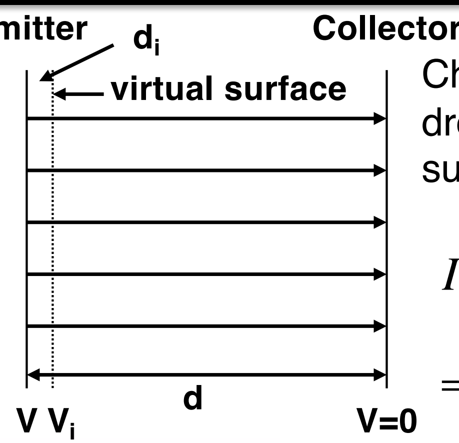

Child-Langmuir solution* + voltage drop between emitter and virtual surface determines current to inject.

$$I = \chi \frac{(V - V_i)^{3/2}}{d_i^2}; \; \chi = \frac{4}{9}\varepsilon_0 \sqrt{\frac{2q}{m}}$$

$$\Rightarrow \Delta Q = Nq = I\Delta t$$

Result

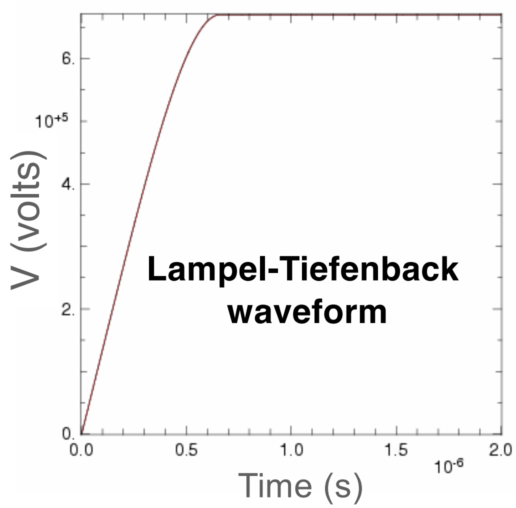

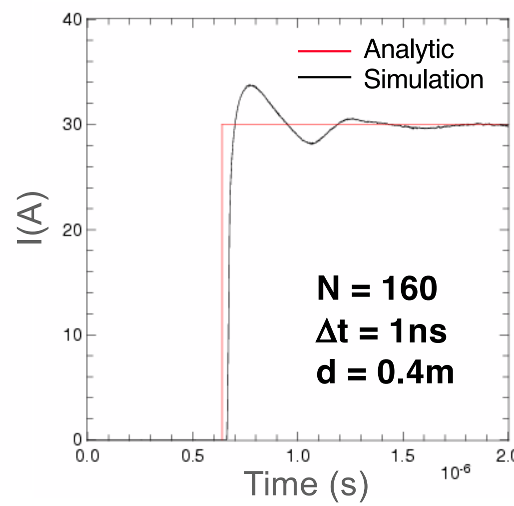

Simulation result exhibits large unphysical oscillation.

*1-D; => J≡I (J=I/S, S=1)

Unphysical oscillation related to Nb particles injected/time step (N_i)

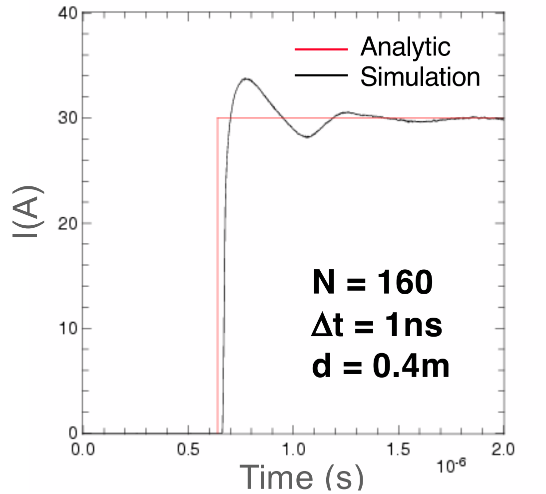

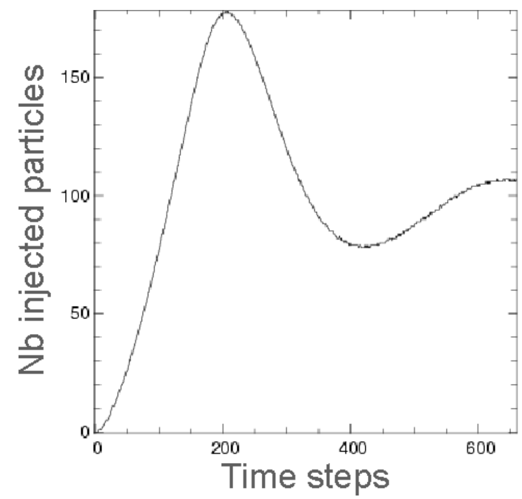

Ideally,

$$\frac{N_i}{\Delta t} = \chi \frac{(V - V_i)^{3/2}}{q d_i^2} = Cste$$

but the driving voltage is a continous function derived analytically.

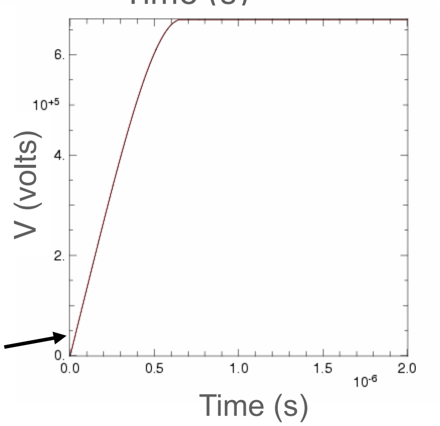

⇒ Inconsistency due to infinitesimal solution applied in discrete world.

Cure: derive voltage history numerically

Injection algorithm

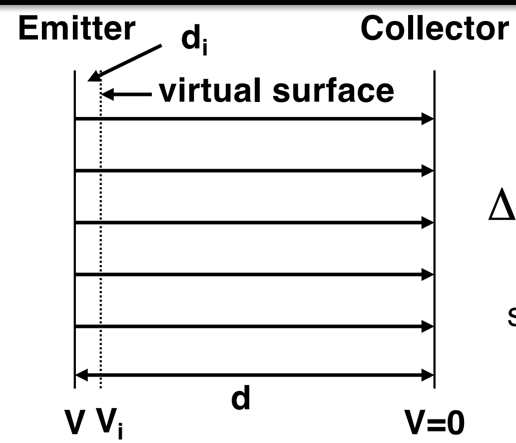

We apply Lampel-Tiefenback method at the discrete level

$$\Delta Q = Nq = I\Delta t \Rightarrow V - V_i = \left(\frac{Id_i^2}{\chi}\right)^{2/3}$$

solve for V using linearity of Poisson

$$(V-V_i) = (V-V_i)_{V=0} + (V-V_i)_{\rho=0}$$

Result

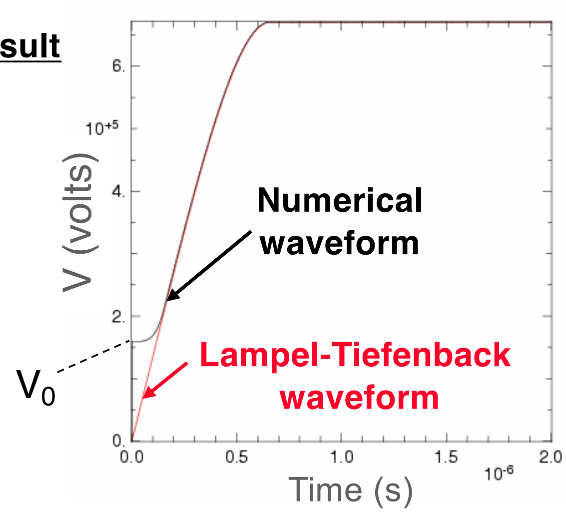

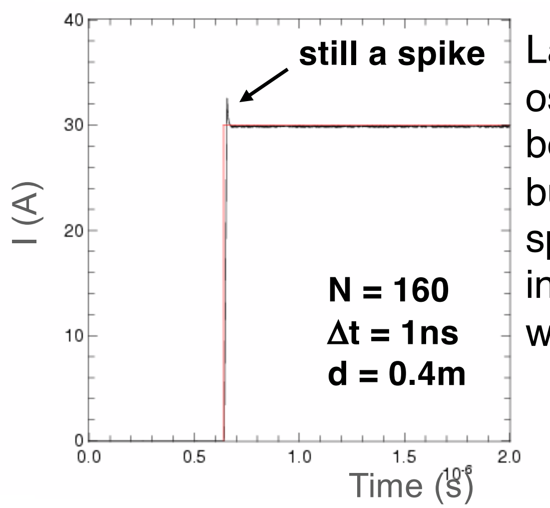

Large unphysical oscillation has been suppressed but there is still a spike. Is it due to initial step V_0 in waveform?

Cure #2: apply irregular gridded patch around emitter.

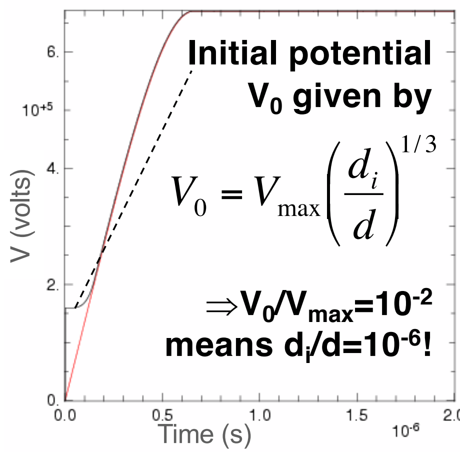

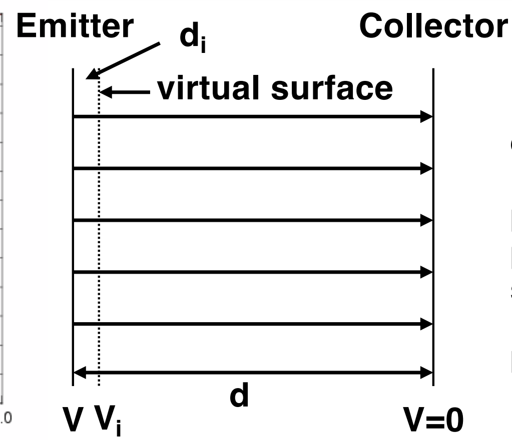

- Apply irregular gridded patch covering d_i
- Mesh sizes such that number of particles per cell is a constant in patch assuming Child-Langmuir solution for $\rho(z)$
- Apply same injection algorithm as before in patch

<u>**Result**</u>

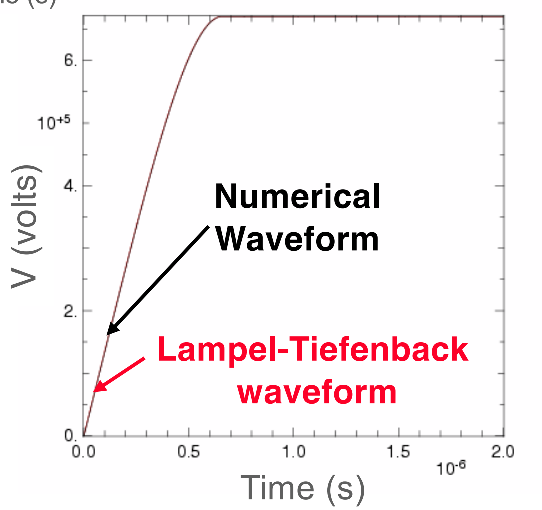

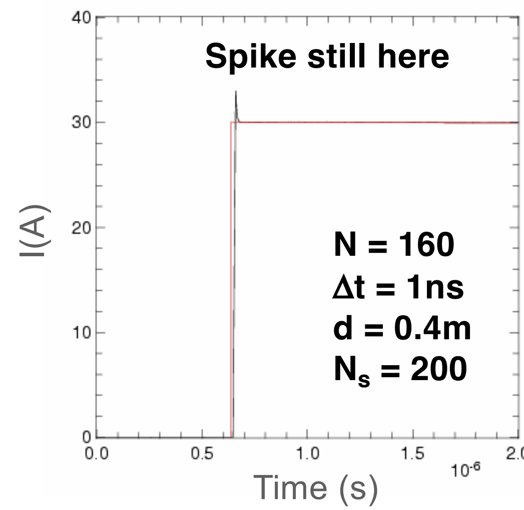

Cure #3: apply regularly gridded patch following front.

An Adaptive-Mesh-Refinement patch
Follows the front

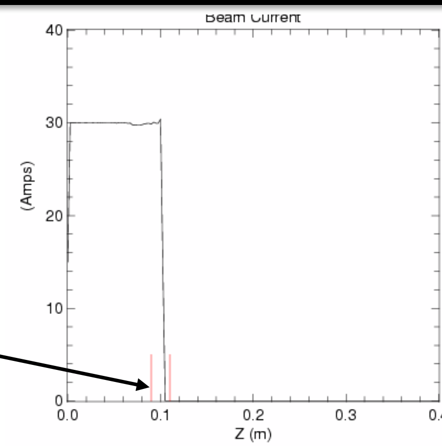

Result

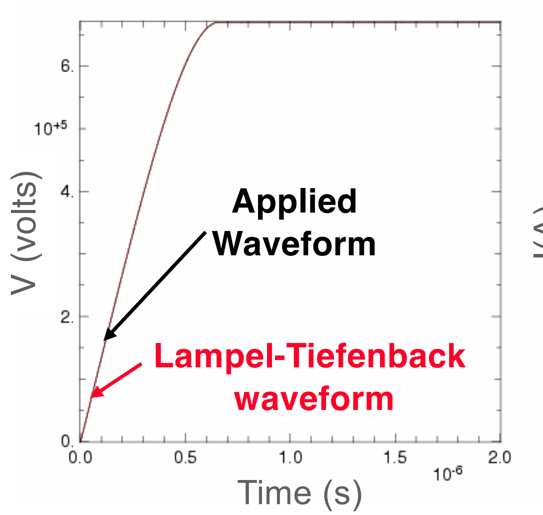

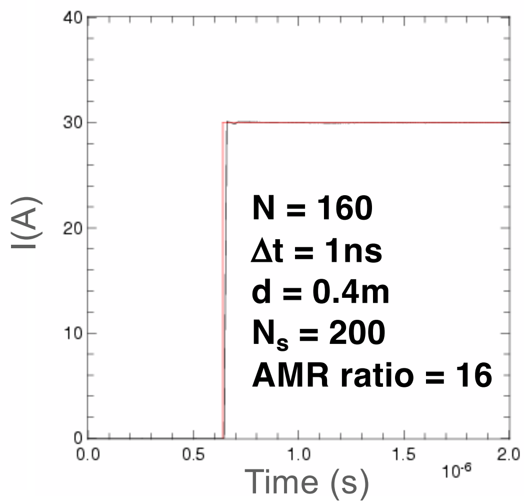

At this point,
we declared
victory!

Extension to three dimensions

- Specialized 1-D patch implemented in 3-D injection routine, as a 2-D array of 1-D patches.

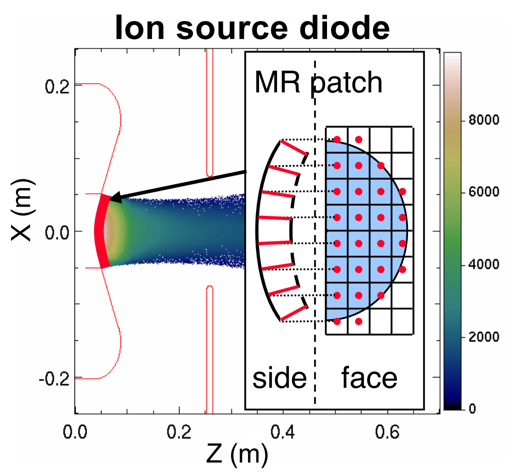

- Extended Lampel-Tiefenback technique to 3-D, and implemented in WARP
  - ➢ predicts a voltage waveform which extracts a nearly flat current at emitter

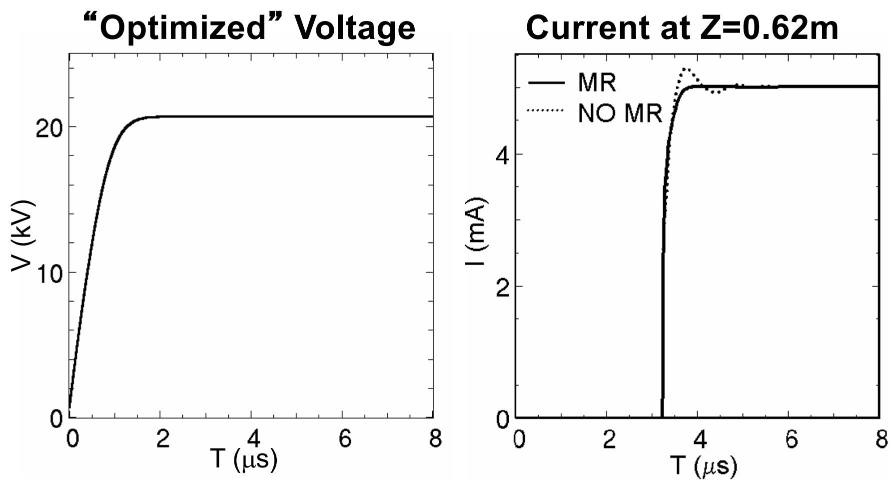

- Without MR, WARP predicts overshoot
- Run with MR predicts very sharp risetime (not square due to erosion)

Test of MR patch on modeling of STS500 Experiment.

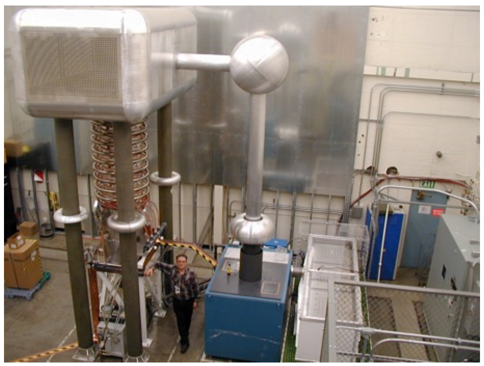

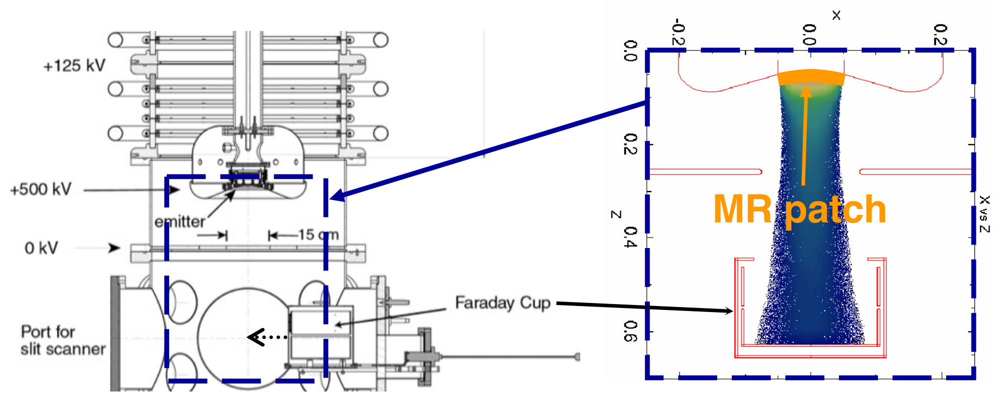

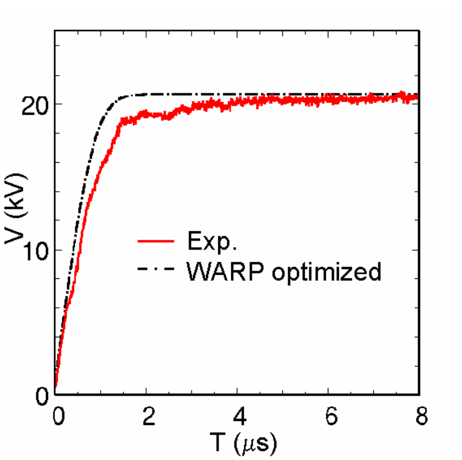

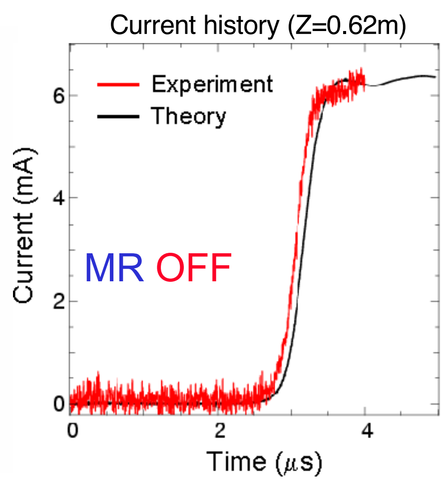

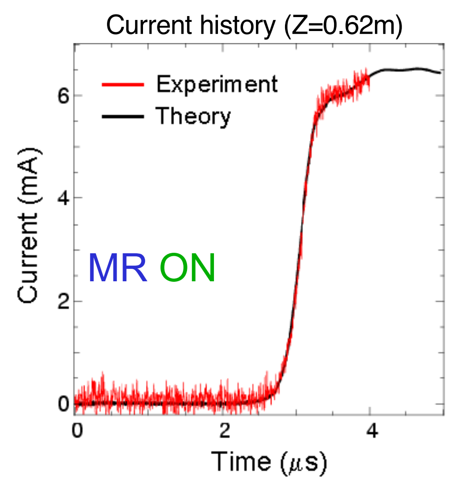

Pierce diode: exercise

① Open Pierce_diode_mrinj.py. Run with w3d.inj_nz = 0, 10, 20 and 100.

② Observe convergence of voltage at t=0 toward 0. Notice very small dz required!

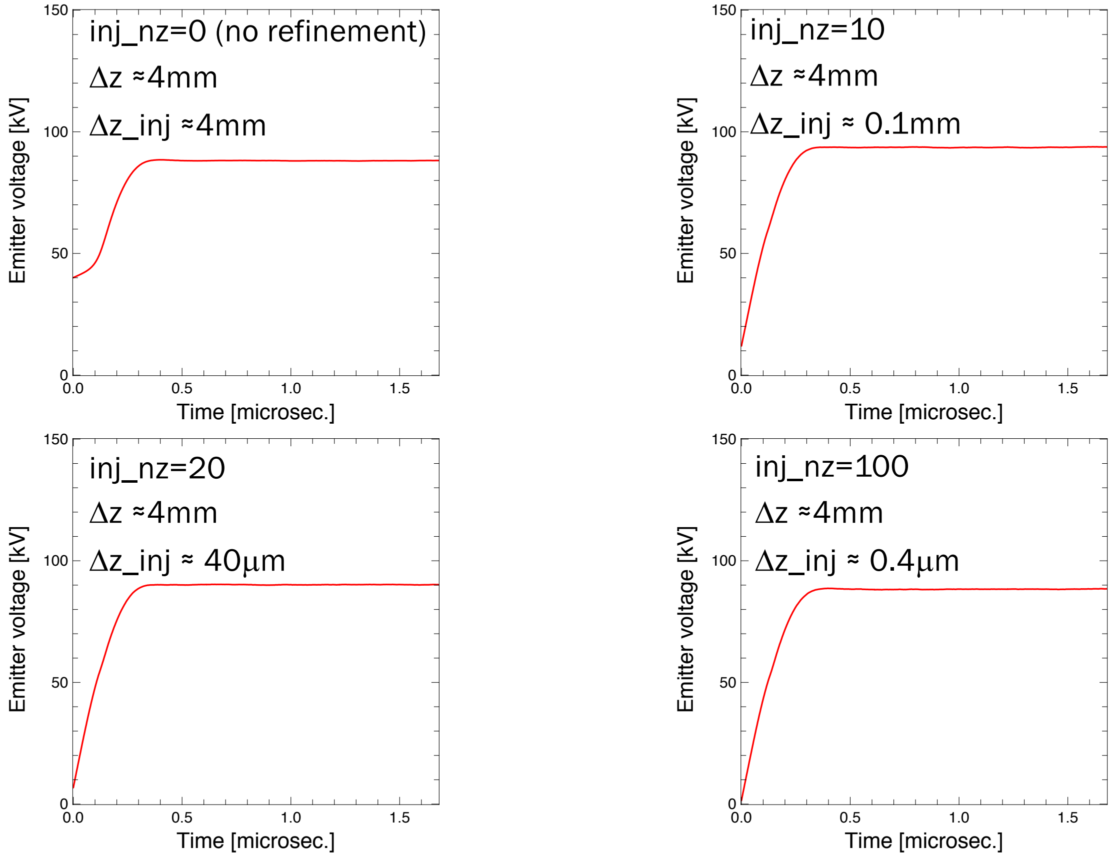

AMR-PIC summary

- Mesh refinement (static or adaptive) can reduce simulation time by several.
- Care is needed to avoid spurious effects (spurious charge & reflections).
- Warp implementation has validated methods, but maintenance is lacking sufficient manpower:

➔ To be used with great care by experience users.

➔ Novel implementation with external AMR package (AMReX) is underway for AMR EM-PIC: WarpX.

References

1. J.-L. Vay, D. P. Grote, R. H. Cohen, & A. Friedman, “Novel methods in the Particle-In-Cell accelerator code-framework Warp”, *Computational Science & Discovery* **5**, 014019 (2012)

2. Vay, J-L.; Friedman, A,; Grote, D.P; “Application of Adaptive Mesh Refinement to PIC Simulations in Inertial Fusion”, *Nuclear Inst. and Methods in Physics Research A* **544**, 347-352 (2005)

3. Vay J.-L., Colella P., Kwan JW., McCorquodale P., Serafini DB., Friedman A., Grote DP., Westenskow G., Adam JC., Heron A., Haber I., “Application of adaptive mesh refinement to particle-in-cell simulations of plasmas and beams” *Physics of Plasmas* **11**, 2928-2934 (2004)

4. Vay J.-L., Colella P, Friedman A, Grote DP, McCorquodale P, Serafini DB, “Implementations of mesh refinement schemes for particle-in-cell plasma simulations.”, *Comput. Phys. Comm.* **164**, 297-305 (2004)

5. Vay J.-L., Adam JC, Héron A, “Asymmetric PML for the absorption of waves. Application to mesh refinement in electromagnetic particle-in-cell plasma simulations.”, *Comput. Phys. Comm.* **164**, 171-177 (2004)